ETH
Eidgenössische Technische Hochschule Zürich
Swiss Federal Institute of Technology Zurich

RSL Robotic Systems Lab
Prof. Dr. Marco Hutter

Master Thesis

Development of sensorized feet for sewer inspection with quadrupedal robots

Autumn Term 2018

Supervised by:
Kolvenbach, Hendrik
Valsecchi, Giorgio

Author:
Ruiz Bassols, Antoni

Declaration of Originality

I hereby declare that the written work I have submitted entitled

Development of sensorized feet for sewer inspection with quadrupedal robots

is original work which I alone have authored and which is written in my own words.[1]

Author(s)

Antoni	Ruiz Bassols

Student supervisor(s)

Hendrik	Kolvenbach
Giorgio	Valsecchi

Supervising lecturer

Marco	Hutter

With the signature I declare that I have been informed regarding normal academic citation rules and that I have read and understood the information on 'Citation etiquette'
(`https://www.ethz.ch/content/dam/ethz/main/education/rechtliches-abschluesse/leistungskontrollen/plagiarism-citationetiquette.pdf`).
The citation conventions usual to the discipline in question here have been respected.

The above written work may be tested electronically for plagiarism.

Zurich, 26.09.2018
Place and date

Toni
Signature

[1] Co-authored work: The signatures of all authors are required. Each signature attests to the originality of the entire piece of written work in its final form.

Intellectual Property Agreement

The student acted under the supervision of Prof. Hutter and contributed to research of his group. Research results of students outside the scope of an employment contract with ETH Zurich belong to the students themselves. The results of the student within the present thesis shall be exploited by ETH Zurich, possibly together with results of other contributors in the same field. To facilitate and to enable a common exploitation of all combined research results, the student hereby assigns his rights to the research results to ETH Zurich. In exchange, the student shall be treated like an employee of ETH Zurich with respect to any income generated due to the research results.
This agreement regulates the rights to the created research results.

1. Intellectual Property Rights

1. The student assigns his/her rights to the research results, including inventions and works protected by copyright, but not including his moral rights ("Urheberpersönlichkeitsrechte"), to ETH Zurich. Herewith, he cedes, in particular, all rights for commercial exploitations of research results to ETH Zurich. He is doing this voluntarily and with full awareness, in order to facilitate the commercial exploitation of the created Research Results. The student's moral rights ("Urheberpersönlichkeitsrechte") shall not be affected by this assignment.
2. In exchange, the student will be compensated by ETH Zurich in the case of income through the commercial exploitation of research results. Compensation will be made as if the student was an employee of ETH Zurich and according to the guidelines "Richtlinien für die wirtschaftliche Verwertung von Forschungsergebnissen der ETH Zürich".
3. The student agrees to keep all research results confidential. This obligation to confidentiality shall persist until he or she is informed by ETH Zurich that the intellectual property rights to the research results have been protected through patent applications or other adequate measures or that no protection is sought, but not longer than 12 months after the collaborator has signed this agreement.
4. If a patent application is filed for an invention based on the research results, the student will duly provide all necessary signatures. He/she also agrees to be available whenever his aid is necessary in the course of the patent application process, e.g. to respond to questions of patent examiners or the like.

2. Settlement of Disagreements

Should disagreements arise out between the parties, the parties will make an effort to settle them between them in good faith. In case of failure of these agreements, Swiss Law shall be applied and the Courts of Zurich shall have exclusive jurisdiction.

Zurich, 26.09.2018
Place and date

Toni
Signature

Preface

First of all, I would like to thank Hendrik Kolvenbach and the Prof. Dr. Marko Hutter for the opportunity given to me to carry out this project in the Robotic Systems Lab. This project stemmed from their initial idea of helping in the subTerranean Haptic INvestiGator project the Robotic Systems Lab is participating in.

I would like to take this opportunity to thank both of my supervisors Giorgio Valsecchi and Hendrik Kolvenbach, they have guided me despite the difficulty of the project. On the one hand Giorgio has been always available to help me and advise me despite being a new member in the RSL and facing his first project as a supervisor and on the other hand Hendrik has been also always willing to help me even after having moved to another country. I think all the meetings with them and all the feedback I got from them have allowed me accomplishing the main objectives of this project.

I would also like to thank all the members of the Robotic Systems Lab for the provided resources and their support during my thesis. I would specially mention Konrad Meyer who has helped me on developing some electronic circuits, has been willing to advise me during the whole project and has explained me how to handle some tools in the lab; and Ruben Grandia who helped me with the preparation of a scratching motion to be performed with the ANYmal's feet.

Moreover, I would like to say that this project would not have been possible without the opportunity that arose to me in my home university ETSEIB-UPC to carry out my Master's Thesis in the ETH-Zurich. For this reason, I would like to thank all the members of the mobility departments in both universities ETSEIB and ETH in order to make this possible.

Finally, I want to thank and dedicate to my family the project that supposes the ending of my Master's degree in Industrial Engineering. Their patience during the hours of work, the help and the support they have provided me have allowed me to get here.

Abstract

The main purpose of the project is to integrate sensors in the feet of the ANYmal, a quadrupedal robot capable of performing autonomous inspections in harsh environments, with the goal of performing sewer inspections included in the subTerranean Haptic INvestiGator project (THING).

The objectives of the project have been divided between: the development of a haptic perception application which allows the ANYmal to differentiate between surfaces while scratching its feet; and the integration of sensors in the ANYmal's feet to perform a water quality analysis in the sewer.

To achieve the desired haptic perception, a foot mockup has been built to test the sensors selected for this application (piezo vibration sensors and an inertial measurement unit). The testing has provided promising results to validate the use of these sensors.

After the results obtained with the foot mockup, these sensors have been integrated in the foot sole of the ANYmal and another a test has been performed, making the foot sole slide manually. The results of this test, again promising, have been verified using the Classification Learner App from the Machine Learning Toolbox of Matlab.

Finally, a waterproof case has been designed to be attached at the frontal right foot of the ANYmal with the purpose of housing all these sensors.

Since the sewer inspection also contains the water quality analysis, another case, which will be attached in the frontal left foot of the ANYmal, has been designed to house the selected sensors capable of measuring properties of the water such as the temperature and the electrical conductivity.

The project has been concluded by performing a scratching motion test with the prototype attached in the feet of the ANYmal.

Therefore, this project contributes to the THING project by giving the ANYmal the possibility of performing autonomous sewer inspections.

Contents

List of Figures

List of Tables

Symbols

Symbols

ϕ, θ, ψ	roll, pitch and yaw angle
b	gyroscope bias
Ω_m	3-axis gyroscope measurement
ω_i	angular velocity in i-axis
μ	mean
σ	standard deviation
μ_s	static friction coefficient
μ_d	dynamic friction coefficient
g	earth gravity magnitude as acceleration unit
a	acceleration
U, V	voltage
C	capacitor
R	resistor

Indices

x	x axis
y	y axis
z	z axis
$piezo$	corresponds to a piezo
H	horitzontal piezo vibration sensor
V	vertical piezo vibration sensor
F	piezo vibration sensor facing to the front of the foot mockup
L	piezo vibration sensor facing to the lateral side of the foot mockup
ard	from the Arduino

Acronyms and Abbreviations

AC	Alternating Current
BOD	Biochemical Oxygen Demand
CS	Chip Select
DO	Dissolved Oxygen

EC	Electrical Conductivity
EPA	Environmental Protection Agency
ETH	Eidgenössische Technische Hochschule
ETSEIB	Barcelona School of Industrial Engineering
FC	Fecal Coliforms
GND	Ground
IMU	Inertial Measurement Unit
LIDAR	Laser Imaging Detection and Ranging
LSB	Least Significant Bit
MISO	Master Input - Slave Output
MPU	Multiple Process Unit
NC	New Concrete
NDT	Non-Destructive Testing
NTC	Negative Temperature Coefficient
OC	Old Concrete
PVDF	PolyVinyliDene Fluoride
RSL	Robotic Systems Lab
SCL	Serial Clock
SCK	Serial Clock
SDA	Serial Data
T	Temperature
TC	Total Coliforms
THING	subTerranean Haptic INvestiGator
UPC	Polytechnic University of Catalonia
USB	Universal Serial Bus

Chapter 1

Introduction

Sewer inspection has become a new problem to face in the last decades, as the sewage system is getting old and it is important to know its conditions in the whole system to discover damages which could pollute the earth surrounding and could be a danger for humans or the natural environment. In several countries it is already determined by law, that pipes must be inspected regularly.

The sewer is a place with inappropriate conditions for the human to work inside: it has a wet and dark environment, variable geometry, poses health risks and the floor can be slippery. However, inspections are needed to see if water quality properties are adequate, to determine the condition of the sewer and to determine if the system is functioning as desired. Any damage in the concrete of the tubes or an excessive quantity of pollutants in the sewer could mean the contamination of the natural environment. Therefore, to prevent man from working in the sewer and still performing quality inspections, a robot can perform all tasks.

In this field the ambition of subTerranean Haptic INvestiGator (THING) [1] project is to advance the perceptual capabilities of highly mobile legged platforms through haptic perception and active exploration. Furthermore, the target for the THING is to perform this exploration in subterranean environments.

The ANYmal [2], as a highly mobile and dynamic quadrupedal robot (Figure 1.1) designed for autonomous operation in challenging and harsh environments, could perform this active exploration in the sewer. The Robotic Systems Lab (RSL) in the ETH together with the City of Zurich, as participants of the project, are working on updating and preparing the ANYmal to perform these explorations.

In the RSL new passive adaptive planar feet with ground orientation and contact force sensing are being developed [3] to improve the mobility of the ANYmal in a wide range of terrains.

Figure 1.1: The ANYmal is a quadrupedal robot designed for autonomous operation in challenging environments.

1.1 Motivation

Now that the new passive adaptive planar feet are being developed, it is the perfect time to adapt them for the THING project towards improving the haptic perception and the active exploration mentioned before.

Different robots have already been used in the sewer to do the visual inspection. However, this project is moving a step forward by including sensors in the feet of the ANYmal to get information about the explored environment.

For sewer inspection and within the THING project's perspective the addition of sensors in the feet of the ANYmal means the possibility to get to know accurately the conditions of the system avoiding the extra effort of placing an operator in it.

1.2 Goals

Following the THING's objective of improving perceptual capability with haptic information and realizing a physical sense of the environment, the purpose of this project is to develop sensorized feet for quadrupedal robots, and more concretely for the ANYmal adapting the passive ankle foot the RSL is currently working on, to perform Non Destructive field Testing (sewer inspections).

The main objective of the project is to develop an application for advanced perception of the surfaces surrounding the ANYmal. Despite the ANYmal is already capable of 3D mapping the environment it is working on thanks to the laser sensors it is using and adapt its movement autonomously according to it, it still does not take into account relevant properties such as the roughness, the compliance or the stability of the surfaces it is surrounded by. According to this, the goal is to develop feet capable of differentiating surfaces or being able to do a terrain classification. This differentiation between surfaces would allow the ANYmal perform more aggressive manoeuvres and help in tasks of surfaces recognition.

In order to develop this application, the goal is to use different sensors integrated within the ANYmal's feet. Due to the small size of these feet, small or micro sensors should be considered and integrated. After the integration, a tool capable of performing the terrain differentiation for the advanced perception should be prepared.

The application mentioned before would help in sewer inspections by determining the conditions of its concrete. Moreover, since the project is focused on the scope of sewer inspections, the secondary goal moves on to integrating all possible components to measure and obtain the sewer's water quality parameters also in the small feet we are working. This water quality analysis would give an extra value to the project and to the possible autonomous inspection the ANYmal could perform in any wet environment.

Chapter 2

State of the art

Sewer inspections are mainly performed using two different procedures: visual inspections, which allow to determine the conditions of the concrete of the sewer looking for flaws, and water quality properties analysis usually performed at the end of big sections of the sewer's line. These procedures have different objectives during the inspection, in this section every procedure is explained in detail and some related work is presented.

2.1 Visual inspection

In the sewer, the flow of water can damage the tunnels. When controlling the damage of the tunnel the inspection company must consider: chemical corrosion, obstacles, sediments, incrustations, erosion, appearance of cracks and deviation of position or deformation of the tubes.

Nowadays, visual inspections are used to detect these flaws and to control the conditions of the tunnel. These inspections are mainly performed with mini video cameras attached to a cable that can record video of a small section of the sewer line (Figure 2.1). This technique is an obstacle to perform fast and autonomous inspections because an operator needs to introduce the camera in the sewer approximately every sixty or hundred meters of pipeline. These small stages lead to the realization of slow and difficult to prepare inspections.

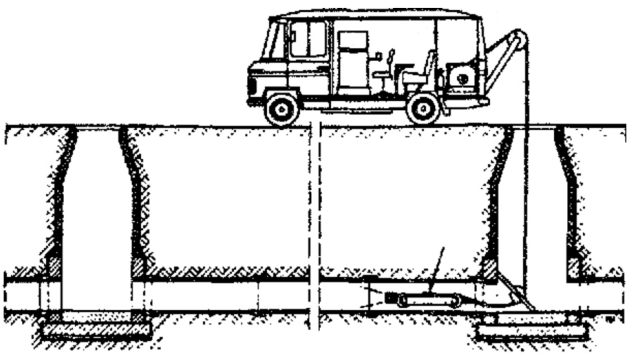

Figure 2.1: Typical system for the visual inspection performed in the sewer.

Moreover, during these visual inspections the camera is normally recording with a quality which could not be satisfactory enough to determine the concrete's status and the videos are normally checked by a sewer's operator, who is the one who decides if the concrete has any damage. Obviously, some image processing can be executed to help with the decisions of the operator but still the conditions of the sewer might not be decent enough for this processing.

Towards avoiding the requirement of an operator to introduce the robot in small stages, some robots have already been developed before (Figure 2.2): the tracked platform RedZone Robotics' Solo [4], the Micro Aerial Vehicle ARSI [5], the IDMind's robot platform in SIAR project as a wheeled robot [6], the water vehicle Spy [7], etc. All these robots have been prepared to perform a visual inspection and in some cases this inspection is already autonomous, but it is only performed using cameras or lasers.

(a) RedZone Robotics' Solo (b) Micro Aerial Vehicle ARSI (c) IDMind's Robot Platform (d) Spy System

Figure 2.2: Developed robots to perform visual sewer inspections.

The ANYmal, with an autonomy of 2-4h, has also the capability of autonomously performing long visual inspections with the cameras and the LIDAR sensor. What's more, as a legged robot it has a flexible mobility and it can easily adapt its movement to all the geometries of the sewer. While doing the inspection, the implementation of the haptic perception can give the robot or the operator more information and can help on determining the conditions of the lines.

2.2 Analysis of water quality properties

As mentioned before, in the sewer it is also important to control the water quality properties in order to correctly perform the water treatment, to avoid polluting the environment and to control the contamination limits of all industries. Normally, measurements are done in the line before the water treatment plant and periodically some laboratory analysis of water samples from different locations of the sewer are performed to get to know the properties of the water locally in possible points of contamination.

Since the ANYmal will be introduced in the sewer for the visual inspection and the haptic perception, it will also be equipped with sensors to measure some water quality properties around the sewer via NDT. This NDT makes possible the performance of fast analysis of these water properties that can or have to be measured in the line. These multiple measurements can also allow controlling more accurately the contamination of the different industrial companies in the water treatment system.

The initial idea is to use the ANYmal in the test zone, the Zurich's sewer. Inside the sewer of a city, domestic wastewater has to be considered in order to control water quality parameters. The sources of pollution in domestic wastewater are:

- Black water: feces, urine, perspiration, water and toilet paper from flush toilets.
- Grey water: water result from washing food, clothing, dishes, as well as from showering and bathing.
- Laundry products: detergents and softeners.
- Cleaning products: disinfectants and bleaches.
- Personal care products: soaps, shampoos, conditioners, sunscreens, deodorants, lotions and oral hygiene.
- Infrastructure: materials, copper pipes, PVC, polyethylene, vitrified clay, hot-water services.

Considering this list of sources of pollution and following the EPA standards [8], the Table 2.1 has been developed to sum up the most important parameters to be considered in terms of water quality for the sewer.

However, not all the parameters shown in the Table 2.1 can be measured in the field. In Chapter 3 it is already made known which parameters have been sensed in this project and which is the selection of sensors that has been done to integrate them in the ANYmal's feet developed by the engineers working on the THING project.

Property, parameter (units)	**Importance**
Acidity, pH (-)	pH adjustment by addition of acidic/basic chemicals allows dissolved waste to be separated from water during the treatment process.
Temperature, T (°C)	Temperature affects water chemistry and the functions of aquatic organisms. It influences the amount of oxygen that can be dissolved in water, rate of photosynthesis by algae, metabolic rates and sensivity of organisms to toxic wastes, parasites and diseases and it can also be an indicator of chemical reactions.
Electrical conductivity, EC (µS/cm)	Saline water conducts electricity more readily than freshwater. As salinity increases, it may become toxic. EC provides a measure of what is dissolved in water, higher conductivity values indicate more chemicals are dissolved in the water.
Nitrates or nitrites, N (mg/L)	Nitrates and nitrites need to be removed or the discharge of the incompletely treated wastewater will cause excess algae growth in rivers and streams.
Phosphorus, P (mg/L)	High concentrations of phosphorus can result in excessive growth of aquatic plants such as cyanobacteria, phytoplankton, macrophytes and filamentous algae.
Biochemical Oxygen Demand, BOD (mg/L)	It provides an index to assess the effect discharged wastewater will have on the receiving environment. The higher the BOD value, the greater the amount of organic matter or "food" available for oxygen consuming bacteria.
Turbidity, Turb (NTU)	Measure of the cloudiness or haziness in water. It can give an idea of the suspended solids (sediments, algaes...) present in the water.
Dissolved Oxygen, DO (mg/L)	The concentration of DO is an important indicator of the health of the aquatic ecosystem because oxygen is essential for almost all forms of life. Oxygen is necessary for respiration and for some chemical reactions.
Oxidation, ORP/Redox (mV)	Alkaline ionized water is an anti-oxidizing agent (negative ORP) and it is able to donate extra electrons to neutralize the harmful effects of free radicals on the body. Most other types of water are oxidizing agents (ORP positive).
Color, Col (Hazen units)	The color of water varies with the ambient conditions and pollution that water presents.
Total coliforms, TC (mg/L)	Coliforms may be associated with the sources of pathogens contaminating water.
Fecal coliforms, FC (mg/L)	The fecal coliform bacteria test is a primary indicator of "potability", suitability for consumption, of drinking water.
Chlorophyll	The concentration of chlorophyll gives an indication of the volume of aquatic plants present in the water column.
Drugs	The presence of drugs in our waterways is a potentially serious environmental and human health issue.
Metal (Cd, Cr, Cu, Ni, As, Pb and Zn)	It is necessary to treat metal-contaminated wastewater prior to its discharge to the environment, since it can cause diseases or health problems.
Level	The level of the water in the sewer might indicate rains or overconsume.
Alkalinity, Alk (mg CaCO_3/L)	Alkalinity is important for aquatic life because it protects or buffers against rapid pH changes.
Fats/Oil/Grease	The fats, oils and grease gradually build up in the sewer network until blockages occur.

Table 2.1: Important parameters to be considered in terms of water quality in the sewer.

Chapter 3

Parameters to be sensed and Sensors selection

The decision of the parameters to be sensed and the selection of sensors has been done after visiting the sewer, carrying out a meeting with the Zurich's sewer operators and developing some research on which sensors could be integrated in the small feet of the robot.

First, the problem has been divided in two parts: on the one hand, some water quality properties must be sensed in the field and, on the other hand, there is the need of developing an advanced perception in the feet of the ANYmal to obtain information about the surrounding environment.

Regarding the water quality properties, which will be sensed in the feet of the ANYmal, these have been selected according to their importance, the way they are measured now and considering the small space available in the feet of the ANYmal. Following these restrictions, the most important parameters are:

- **Physical properties**: temperature and haziness.
- **Chemical properties**: pH, electrical conductivity, nitrogen, phosphorus and dissolved oxygen.

It is not possible to measure all these parameters in the field. Parameters such as nitrogen, phosphorus or dissolved oxygen are normally quantified after laboratory water samples analysis. However, techniques such as infrared spectroscopy have already been developed to measure these chemical properties in the field. Nevertheless, the existence of small spectrosmeters is still limited, and it is impossible to integrate them in the feet of the ANYmal. One example could be the SCiO hand-held spectroscometer [9] in Figure 3.1. Despite these new techniques, the selected parameters to be sensed in the sewer are: temperature, acidity or pH and electrical conductivity.

Indeed, haptic perception is the main objective of the project and some sensors must be included to perform it. In addition, to give more value to this project the possibility of integrating a sensor to detect some kind of material was considered. Since in the sewer metal objects can be found and can cause the malfunction of the system, a metal detection sensor has been considered.

Finally, taking into account that the feet of the ANYmal can be considered as a solid block, without intern space to include the sensors, an add-on will have to

Figure 3.1: SCiO hand-held spectroscometer.

be created without overcoming the space limitation. In these add-ons, the sensors that will be included are the ones included in the diagram, in Figure 3.2, which summarizes the most important parameters and applications to be considered and includes the decision done for the sensors.

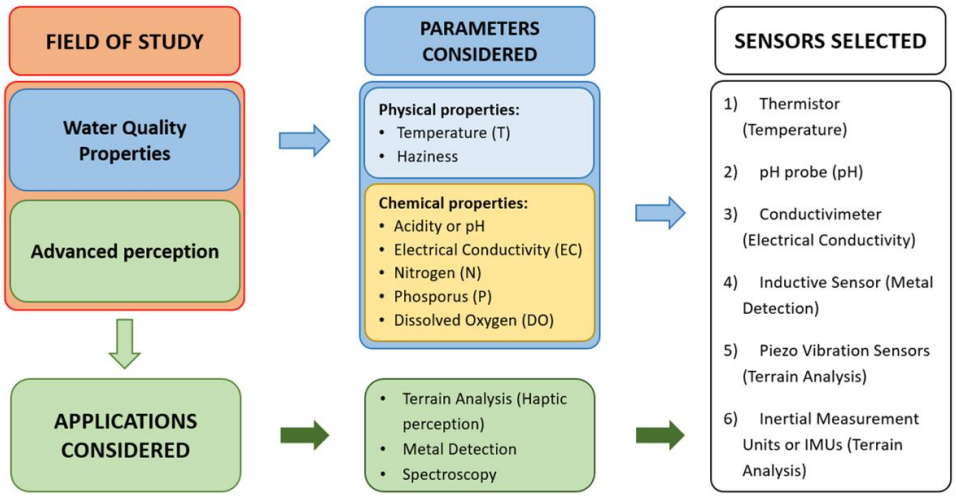

Figure 3.2: Diagram that summarizes the research done, towards the sensors selected, according to the parameters and the applications considered in the field of study.

Therefore, basically the small dimension has been the most important property to follow when selecting all the sensors. Finally, as can be seen in Figure 3.2, the sensors selected to be included in the feet of the ANYmal are the following:

1. **Thermistor**: resistor whose resistance is dependent on temperature. Generally the material used in a thermistor as a variable resistor is a ceramic or a polymer.

2. **pH probe or pH meter**: scientific instrument that measures the hydrogen-ion activity in water-based solutions. It indicates the acidity or alkalinity of the water expressed as pH.

3. **Conductivimeter or electrical conducitivity meter**: scientific instrument, normally a probe, that measures the electrical conductivity in a solution. Generally, the principle used is the reading of the voltage between electrodes.

4. **Inductive proximity sensor**: instrument that can detect metal targets approaching the sensor, without physical contact with the target. It is based on Faraday's law of induction.

5. **Piezo vibration sensors**: electronic component suitable for measurements of flexibility, vibration, impact and touch. The principle of the sensor is the creation of an AC voltage while vibrating.

6. **Inertial Measurement Unit (IMU)**: electronic component that measures the accelerations and angular velocities using the combination of an accelerometer with a gyroscope.

It is clear how useful each sensor can be except for the piezo vibration sensors and the IMU; the idea of using these sensors is to use the information of the absorbed forces and from the movements of the feet while starting contact with the surrounding surfaces or while developing a scratching motion in these surfaces with the feet of the ANYmal.

In Chapters 4 and 6 the specific sensors used are introduced and their integration is explained accurately.

Chapter 4

Terrain Analysis Application - Haptic Perception

In sewer inspection, the conditions of the concrete in the sewage system are the most important thing to take into account. In order to improve the haptic perception of the ANYmal, the idea is to create an application capable of differentiating between the status or properties of the surrounding surfaces.

To reach this goal, the concept we have worked on is to use one foot of the ANYmal: make it slide on the surface performing a scratching motion; and by reading the data from the IMU and the piezo vibration sensors get to know this surface or its properties. This would allow differentiating between surfaces or in the sewer's case the conditions the concrete. With this concept, by sliding the feet the roughness or friction of the ground could also be recognized.

This concept has been already developed with an IMU in [10] trying to emulate a surface roughness test and in [11] with pressure sensors. In order to achieve our goal the sensors selected, included in Figure 4.1, have been:

- **SparkFun Triple Axis Accelerometer and Gyro Breakout - MPU-6050**: this device combines a 3-axis gyroscope, a 3-axis accelerometer and a Digital Motion Processor all in a small 4x4x0.9mm package. Its features are:
  - I2C Digital Output of 6 or 9-axis MotionFusion data.
  - Input Voltage: 2.3 - 3.4V.
  - Selectable Solder Jumpers on CLK, FSYNC and AD0.
  - Tri-Axis angular rate sensor (gyro) with a sensivity up to 131 LSBs/dps and a full-scale range of ±250, ±500, ±1000 and ±2000 dps.
  - Tri-Axis accelerometer with a programmable full scale range of ±2g, ±4g, ±8g and ±16g.
  - DMP engine offloads complex MotionFusion, sensor timing synchronization and gesture detection.
  - Embedded algorithms for run-time bias and compass calibration. No user intervention required.
  - Digital-output temperature sensor.
  - 1 x 0.6 x 0.09" (25.5 x 15.2 x 2.48mm).

- **LDT0-028K Piezo Vibration Sensor - Large with Mass**: this piezo sensor from Measurement Specialties is often used for flex, touch, vibration and shock measurements. It can create an AC voltage up to +/-90V when the film moves back and forth. It could also be used for impact sensing or a flexible switch. This version includes a mass to increase the sensivity to motion. Its features are:
  - Flexible PVDF Piezo Polymer Film.
  - Wide dynamic range.
  - Laminated for higher voltage output.
  - 0.1" breadboard friendly leads.

(a) LDT0-028K Vibration Sensor (b) MPU-6050

Figure 4.1: Sensors included in the foot mockup.

With the purpose of testing these sensors, before integrating them in the feet the RSL was working on, a foot mockup has been designed with the ambition of already being able to differentiate surfaces with it.

4.1 Foot Mockup

Remembering that the way we want to improve the haptic perception is by getting data from sensors while developing a scratching motion with the feet of the ANYmal; a foot mockup, oversizing the dimensions of the real feet and with the goal of testing the IMU and the piezo vibration sensors, has been built in.

The foot mockup sole has been designed according to the real foot sole dimensions of the ANYmal (90x58mm). From here, the design has been done considering all the possible configurations the piezo vibration sensors coculd be installed. For this reason, the foot mockup is a cube in which it is possible to integrate a prototyping board inside in all its faces with the piezo vibration sensors connected facing different directions.

The creation of the design, included in Figure 4.2, has followed these requirements:

1. It should include the possibility of integrating a 70x70mm prototyping board in all the intern faces of the cube.

2. It should include lateral slots to work manually inside.
3. A cover should be designed with the purpose of integrating an Arduino UNO board on the cube.
4. Metal pieces should be attached with the purpose of having at least a force of 10N against the ground allowing to emulate a scratching motion by sliding the cube.
5. The rubber under the sole should have the same dimensions as the rubber under the real foot sole (90x58mm).
6. It should include some wholes where to tie a rope in order to pull the cube and make it slide manually.

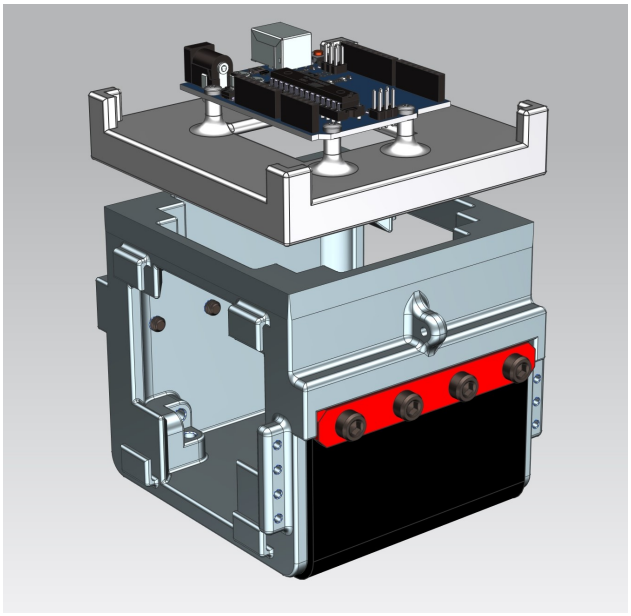

Figure 4.2: Assembly model of the designed foot mockup. This foot mockup has been used to test the IMU and the Vibration sensors towards the goal of haptic perception.

The final design, included in Figure 4.3, includes: the Arduino UNO attached on the cover, the prototyping board with the vibration sensors, the IMU attached on the cube's base, the metal pieces attached in the front and the back part of the cube, the rope tied in the front ready to pull and make the cube slide, the sole with adapted dimensions and all the wires and connections done. The foot mockup has the following features:

- Dimensions: 104 x 110 x 115mm
- Weight: 1450g

In Figure 4.3, it is shown that the initial configuration for the piezo vibration sensors include four of these sensors, this way a comparison can be done between them. Moreover, two of the vibration sensors are facing forward while the other two are facing to the lateral. Some initial tests were performed before the test explained in next Chapter 5 in order to find the best configuration. The chosen configuration installed in the foot mockup was selected because its easy installation and because

the signals obtained with the vibration sensors were giving the highest amplitude of all different possible configurations.

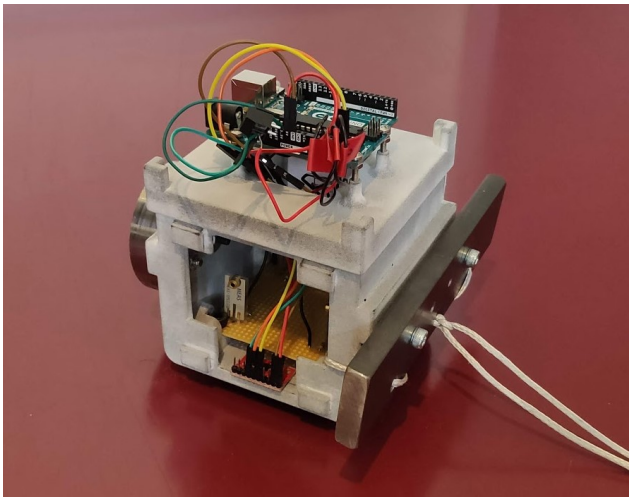

Figure 4.3: Foot mockup integration ready to be tested by sliding it on different surfaces.

Chapter 5

Experimental tests with the foot mockup and Data analysis

Once the foot mockup has been built, the following step has been the design of the electronic circuits for all the integrated sensors (4 piezo vibration sensors and the IMU in the foot mockup). And then, a code, for the correct operation while measuring the data with the sensors, for the Arduino UNO has been prepared.

After the whole preparation has been concluded, two different tests have been performed: the first test with the goal to verify if with the use of this haptic application it is possible to differentiate between surfaces; and the second test, already in the sewer, in order to check which behavior has the application in the same kind of surface, in this case the concrete of the sewer, but with different conditions (age, humidity, erosion...).

5.1 Electronic circuits

One the one hand, the circuit for each of the piezo vibration sensors, included in Figure 5.1, consists in using a high value resistor (R_c) of 10MΩ in parallel with the sensor represented with an AC voltage source and a capacitor. Moreover, since the sensor creates an AC voltage and the Arduino, with the analog inputs (A_i) is only capable of reading voltages between 0 and 5 volts, there is the need of centering the signal at 3.3V to read the negative voltage.

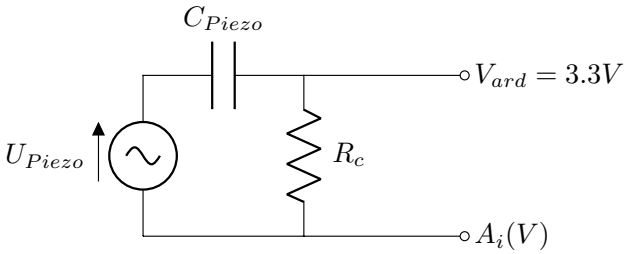

Figure 5.1: Electronic circuit used to integrate the piezo vibration sensors.

On the other hand, the circuit for the IMU is the one included in Figure 5.2. The circuit has been obtained from its datasheet A.1.

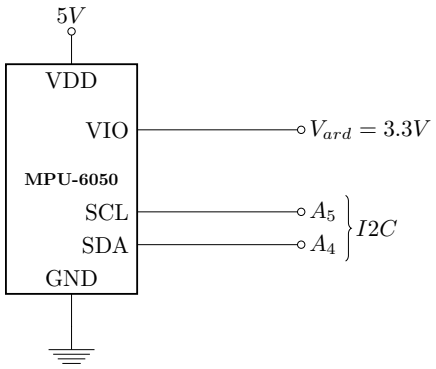

Figure 5.2: Typical operation circuit for the IMU MPU-6050.

The code used to read the signal from these sensors is the one included in Appendix B.1. It has been adapted according to the number of vibration sensors used.

5.2 Data analysis

Before introducing and explaining in detail every test, it is necessary to explain how we have reached the results shown at next sections.

The data obtained, using the circuits and the code mentioned in the last section, contains time series for each of the variables read. Within this set of temporal series, we have worked with three types of variables:

- AC voltage from the vibration sensors.
- Acceleration obtained with the IMU in all three axis.
- Angular velocity obtained with the IMU in all three axis.

Initially, the adaptation of the signals provided for each of the three variable types is needed:

1. In the case of the voltage from the vibration sensors, it is initially centered at 3.3V because of the circuit imposed to read the negative voltage from the AC created with the Arduino. Consequently, there is the need of centering this signal at 0V to obtain temporal series centered at 0V. In Figure 5.3 an example of voltage time series centered at 0V is included.

2. In the cases of the 2 different types of variables obtained with the IMU, if the sensor is initially well calibrated there is only the need of transforming the LSB units of the acceleration and the angular velocity to normal units for these physical variables. Therefore, there is the need of realizing the following transformations:

$$a(g) = a(LSB)/16384 \tag{5.1}$$

$$\omega(^\circ/s) = \omega(LSB)/131 \tag{5.2}$$

   In the case of the acceleration in z-axis 1g has been substracted in order to center it at 0g. In Figures 5.4 and 5.5 examples of acceleration and angular velocity time series are included.

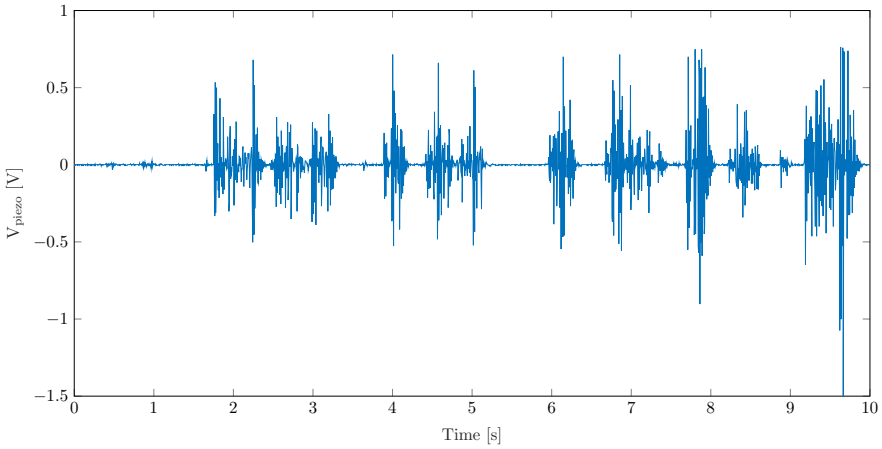

Figure 5.3: Time series of the voltage created with a piezo vibration sensor.

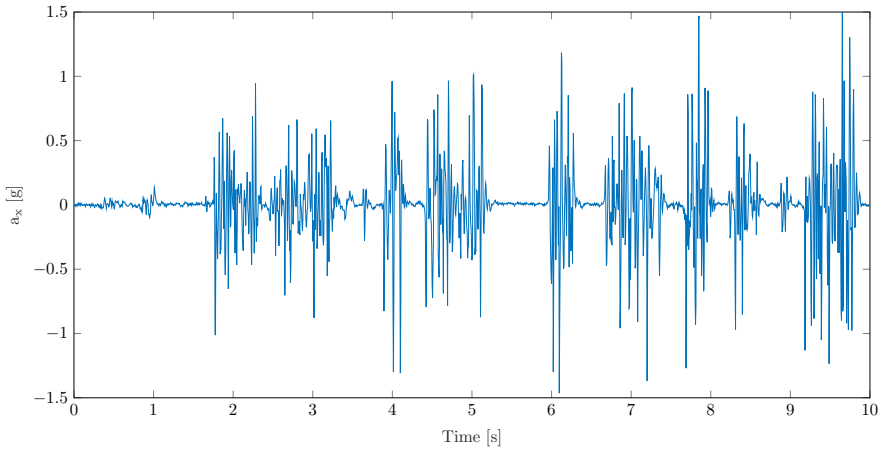

Figure 5.4: Time series of the acceleration in x-axis measured with the IMU.

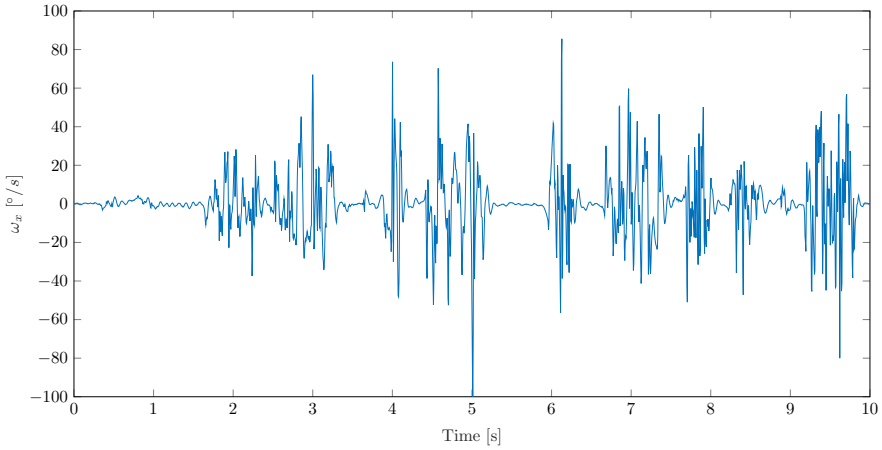

Figure 5.5: Time series of the angular velocity in x-axis measured with the IMU.

Once the signal of each variable has been adapted next steps have been followed:

1. The normal distribution that represents each variable in its time series has been obtained. In Figure 5.6, it is possible to see an example how the signal obtained for these variables follow a normal distribution.

2. From the normal distribution obtained the mean (μ) it is always a value around 0 because all signals at centered at 0. Therefore, the value that is giving information about each of the time series is the standard deviation (σ).

3. To make this value more representative, the 95% confidence interval of the normal distribution is obtained with:

$$95\%IC = (x_{min}, x_{max}) = (-1.96\sigma, 1.96\sigma) \tag{5.3}$$

   where x is the variable and σ is the standard deviation calculated. The value obtained that limits the 95% Confidence Interval is considered as the maximum value that this variable would obtain while sampling with same conditions.

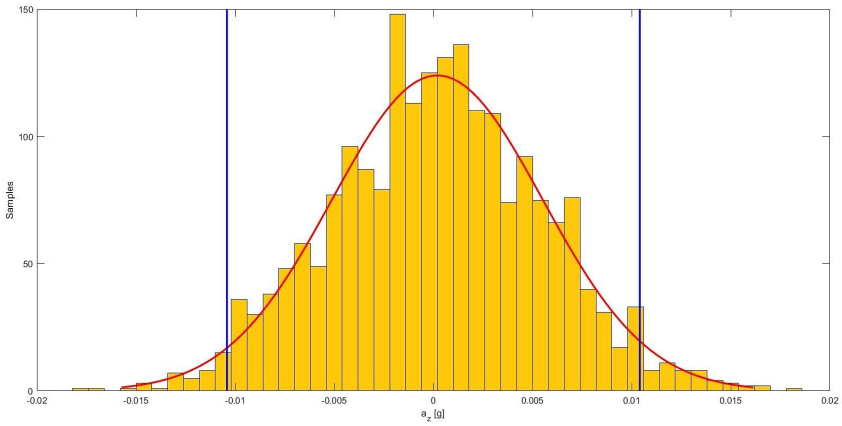

Figure 5.6: Normal distribution of the z-axis acceleration from the IMU with the 95% confidence interval limited with blue lines. The data in yellow has been obtained sliding the cube in a random surface.

4. Since in all the tests more than a sample is taken in each surface, an average of all the limiting values of the 95% confidence interval has been calculated to make the result more reliable.

5. Finally, from the results obtained a Spider chart is fulfilled with the considered maximum value for all the variables measured (voltage from the piezo sensors, acceleration and angular velocity from IMU in all axis) in all different surfaces, the maximum value obtained in all surfaces for each parameter has been taken as reference for limiting the spider chart. The Spider chart as can be seen in Figure 5.7, allows you to easily see how the results are and compare between surfaces.

This Spider chart representation has been adapted in each of the following sections and chapters according to the number of piezo vibration sensors used and the number of surfaces studied in each of the tests.

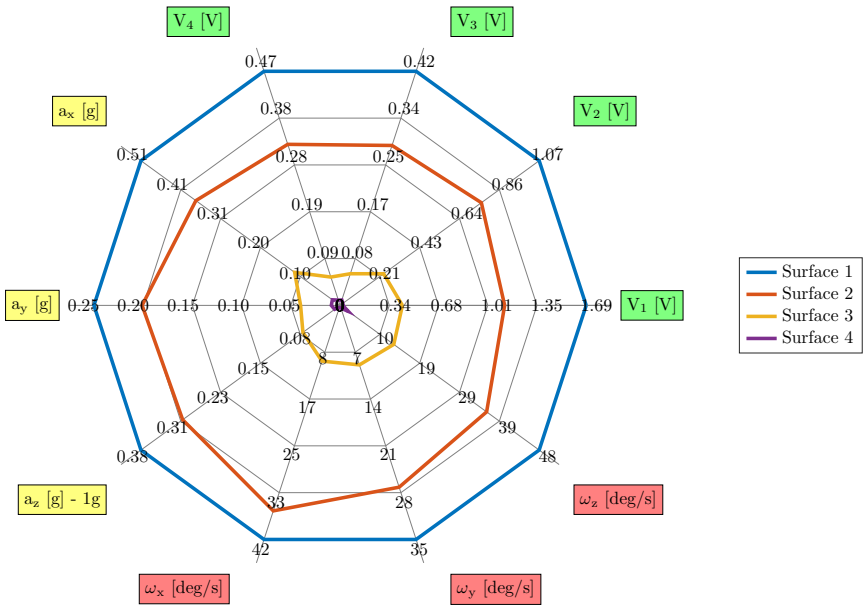

Figure 5.7: Spider chart where all the parameters read are represented (in this case four voltages created with the vibration sensors and acceleration and angular velocity in all axis measured with the IMU) within each of the different surfaces sampled (in this case four random surfaces).

5.3 Different surfaces - Foot mockup test

Once clarified the way the analysis it is done, the tests have been performed. First, in order to validate the haptic perception obtained, using piezo vibration sensors and an IMU, while performing a scratching motion with the feet of the ANYmal a test has been performed with the foot mockup. The idea for this test is to see if by sliding the cube in different surfaces, after the analysis, it is possible to differentiate between surfaces.

For this reason, during the test, the foot mockup has been slid in four different surfaces (Figure 5.8): gravel, rough asphalt, track and smooth flat. All the data generated with the sensors has been saved using a software called CoolTerm [12] capable of saving what is written in the serial port terminal of the Arduino.

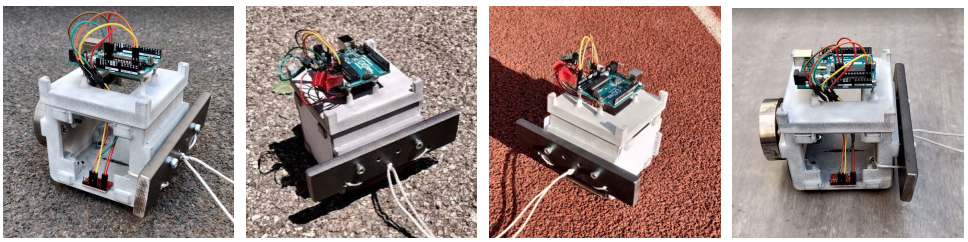

(a) Gravel (b) Rough Asphalt (c) Track (d) Smooth Flat

Figure 5.8: Foot mockup standing in all the different surfaces where samples have been taken for the Different surfaces test: gravel, rough asphalt, track and smooth flat.

As mentioned before ten variables have been read in this test with the foot mockup: 4 AC voltages from the piezo vibration sensors and acceleration and angular velocity in all axis (x, y, z) from the IMU. To make an initial comparison between surfaces, the time domain of these variables has been plotted and already with the amplitude of the signal obtained it is already visible that every sample correspond to a different surface. In Figure 5.9, as an example, I have plotted the time series of the acceleration in z-axis in one sample of each all different surfaces; it is possible to differentiate surfaces only by taking a look at the amplitude of the signal.

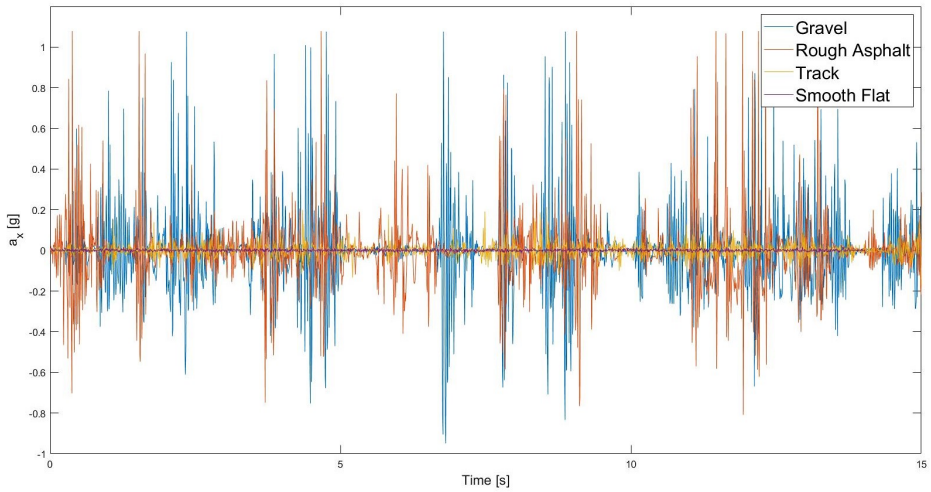

Figure 5.9: Time series of acceleration in z-axis while sliding the cube on the surfaces of gravel, rough asphalt, track and smooth flat.

By taking a look at the graph plotted, the amplitude of the signal is the one expected for every surface. While sliding the cube on gravel or rough asphalt, the roughness of the surface causes the appearance of acceleration or angular velocity when the cube is moving because of the behavior of the rubber while touching the surface. In the case of the track and the smooth flat since the surface is smoother the rubber can slip easily and less vibrations or accelerations appear in the movement.

In order to validate the suspected results, the analysis following the steps explained in last section has been done. The obtained spider chart (Figure 5.10) includes: V_{F1} and V_{F2} as the voltage from the vibration sensors facing to the front of the foot mockup; V_{L1} and V_{L2} as the voltage from the vibration sensors facing to the sides of the foot mockup; a_x, a_y, a_z from the IMU's acceleration in all axis; and ω_x, ω_y and ω_z from the IMU's angular velocity in all axis.

This spider chart makes clear that the amplitude of the signals allows to differentiate between surfaces, through the use of these sensors, in a scratching motion on the ground. Visually the results obtained show that more vibrations and accelerations are created respectively in gravel, rough asphalt and track than in smooth flat surfaces. It also shows that the parameters of more amplitude as expected are the ones which consider the x-axis (the direction of the movement) and the z-axis (the direction perpendicular to the ground and the movement).

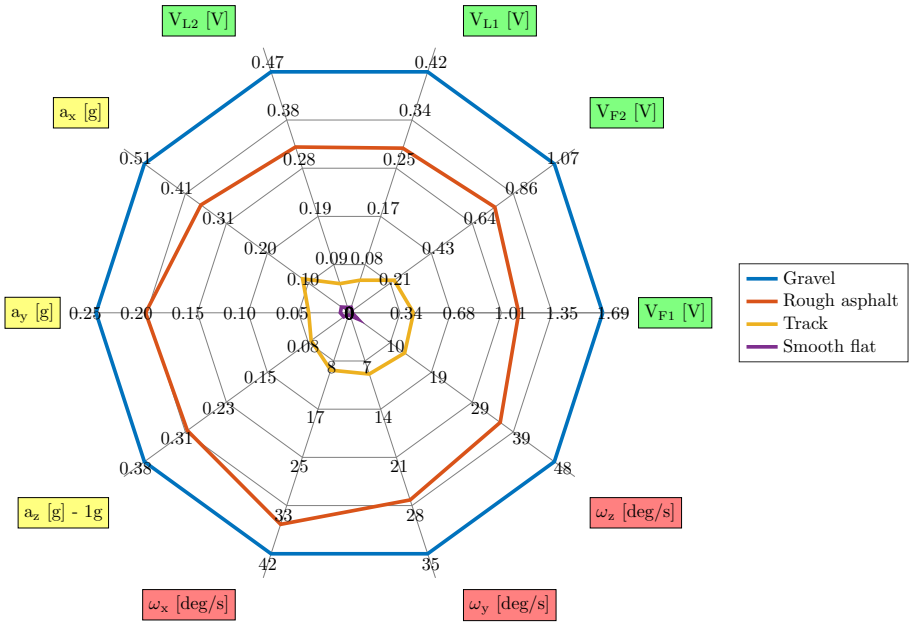

Figure 5.10: Spider chart that allows to make a visual comparison between the results obtained with the ten parameters measured while sliding the foot mockup on four different surfaces: gravel, rough asphalt, track and smooth flat.

5.4 Sewer's concrete status - Foot mockup test

The main objective of the project and to give a value for advanced perception within the THING's project perspective was to achieve an application that is capable of differentiating between surfaces according its conditions. In sewer inspections this would help because differentiating between concrete in good and bad conditions, just by scratching the surface with the feet of the ANYmal, could avoid the introduction of the sewer's operator into it.

Therefore, this initial test in the sewer with the foot mockup (cube), with the IMU and the vibration sensors, had the goal of seeing if with this application we can detect erosion in the concrete just by sliding the cube on it.

In the sewer (Figure 5.11), the way the data was obtained might not be the best because of its conditions. However, after installing a lateral cover to make splashproof the cube, different samples were taken manually in different sections of the sewer according to the operator's experience.

The sampling was done mainly in two different sections of the sewer: the first section was an old section with eroded concrete and the second one was built or renewed a few years ago. In both sections the data was taken from three different zones:

- **Central zone**: water flows there continuously.
- **Intermedium zone**: normally wet but water only flows there when the level slightly increases.
- **Side zone**: the level of the water needs to increase enough to reach this zone, for example after rains or overconsume.

Figure 5.11: Picture while manually taking samples in the sewer with the foot mockup.

For every different zone three samples were taken in order to make the test more reliable.

Again, since the sensors used were four piezo sensors and an IMU ten parameters were considered for the analysis: 4 AC voltages created for the piezo vibration sensors (two $V_F(V)$ for the piezos facing to the front and two $V_L(V)$ for the piezos facing to the lateral side of the foot mockup) and the acceleration and the angular velocity in all directions (x, y, z). After following the analysis explained in Section 5.2 the results obtained in next sections are confident enough.

As a counterpart, it is necessary to say that the way the data was obtained might not be the best by sliding the cube manually, trying to have a constant and the same velocity in every sample with the conditions present in the sewer. Moreover, since it is an initial analysis the sewer has been considered as flat, to get still better results the small slope of the ground in the sewer should be considered continuously.

5.4.1 Old concrete

Initially for the Old Concrete (OC), it is easy to see that the most eroded part is the one where water flows continuously. It is also possible to see that while approaching the side of the sewer there is a decrease of the maximum values of all the parameters measured meaning that the sewer is not being eroded homogeneously. The results have been plotted in next Figure 5.12.

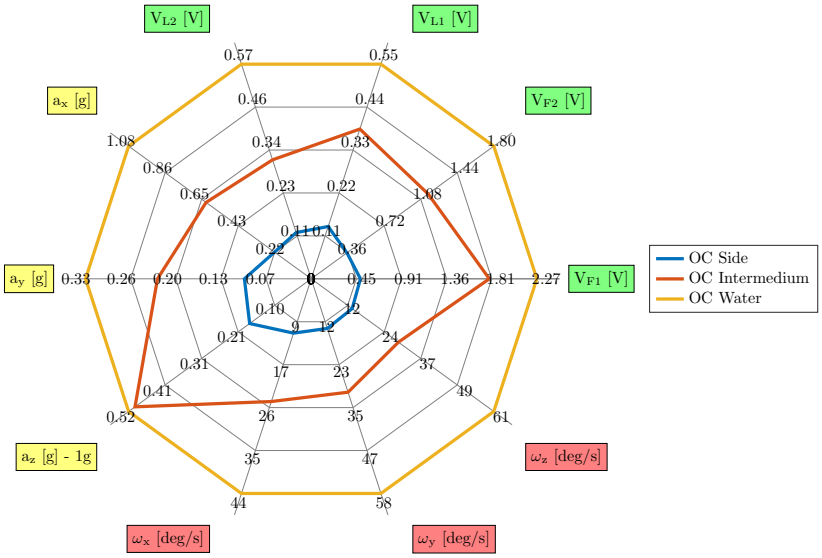

Figure 5.12: Spider chart that contains the results of the analysis done with the parameters measured, in different zones of the sewer, in the old concrete section.

5.4.2 New concrete

In the second concrete section (reNewed Concrete) (NC) the lack of erosion doesn't allow to differentiate clearly between the three different zones and the results plotted in Figure 5.13 are not trustworthy.

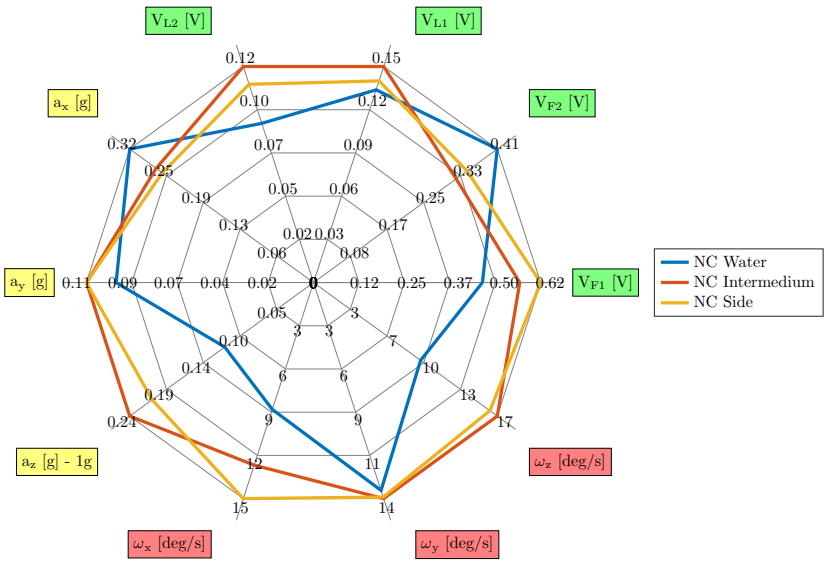

Figure 5.13: Spider chart that contains the results of the analysis done with the parameters measured, in different zones of the sewer, in the new concrete section.

5.4.3 All concretes and friction coefficients

If we compare the two sections, plotting all results in one spider chart (Figure 5.14), of the sewer we can see that the new concrete results are similar to the side zone (less eroded) results in the old concrete. In addition, we can see how the water affects at least in the measurement of the acceleration in the z axis, the value expected out of the water is much higher, if we take as reference the measurement in the old concrete with water (like it has been done in the spider chart).

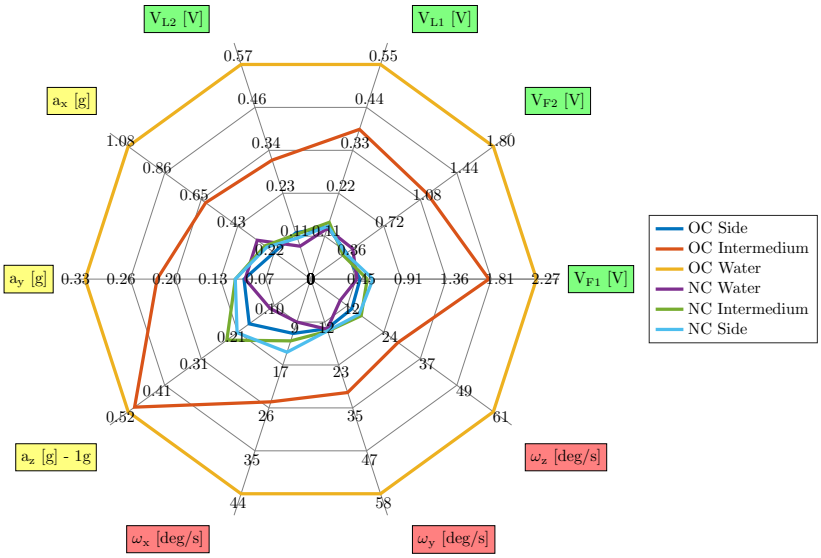

Figure 5.14: Spider chart that contains the results of the analysis done with the parameters measured, in different zones of the sewer, in both the new and the old concrete section.

Since saples were taken in the sewer, a dynanometer was used in order to measure and get values for the static (μ_s) and the dynamic (μ_d) friction coefficients. These values are important for the ANYmal's control and to develop correctly the scratching motion with the feet. Considering the mass (m) of the foot mockup is 1,4 kg and the force needed to initiate the movement(F_s) was 0,75kg the static friction coefficient is around 0,54 and for the dynamic the force needed (F_d) was 0,65kg so the dynamic friction coefficient is around 0,47. Those coefficients have been calculated using next equations:

$$\mu_s = F_s/m \tag{5.4}$$

$$\mu_d = F_d/m \tag{5.5}$$

This test, has verified that the sensors used (IMU and Vibration sensors) are valid to perform a haptic perception to get to know the roughness of the surrounding surfaces and differentiating them by scratching the feet of the ANYmal on them. Moreover, this new haptic perception developed can give the ANYmal the opportunity of realizing the sewer inspection by itself and it open many doors to other kind of applications (soil texture inspections, road flaws inspections...). In Chapter 6 these sensors have already been integrated in the feet of the ANYmal together with the sensors selected for the water quality analysis.

Chapter 6

Integration of the electronic circuits in the feet

The integration in the feet of the robot has been performed trying to avoid any kind of loss of mobility with the ANYmal. Since the natural behavior of the robot while inspecting is walking forward, the decision of integrating the sensors in the frontal feet of the robot has been done. For this reason, the sensors have been installed in the exterior part of the frontal feet of the robot leaving the possibility of still adding sensors in the rear feet. Moreover, the control and reading of the sensors has been done with an Arduino UNO integrated in a splashproof box in each shank of the frontal legs. In next Figure 6.1, it is included the design of the passive ankle used in this project.

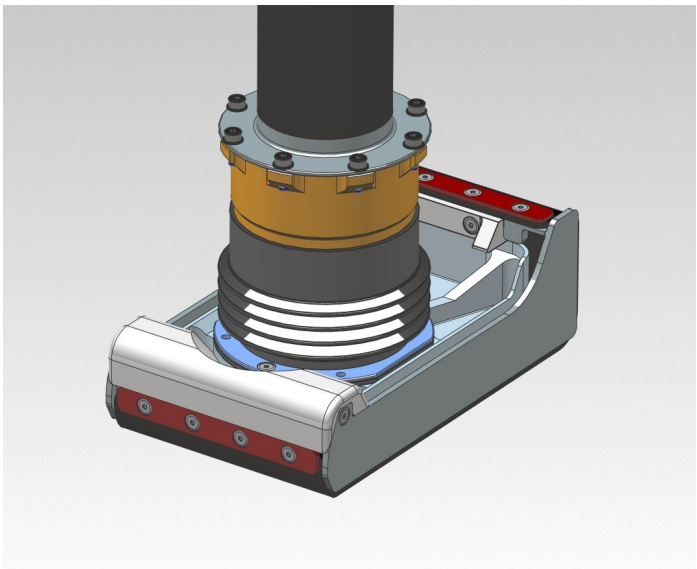

Figure 6.1: Design of the passive ankle including foot sole and part of the shank.

Therefore, the following integration has been carried out:

Frontal Right Foot Terrain Analysis Application

- IMU
- Piezo Vibration Sensors

Frontal Left Foot Water Quality Parameters Analysis

- Thermistor
- Conductivimeter
- pH-meter
- Inductive Sensor

The initial design, to house the sensors and the electronic circuits needed in each foot, is the lateral case included in the Figure 6.2 already attached in the foot sole. From the point of view of the THING project this case should be waterproof, it should not be wider than 25mm, it should have a clearance with the floor of at least 5mm and its height should not be higher than the height of the foot sole.

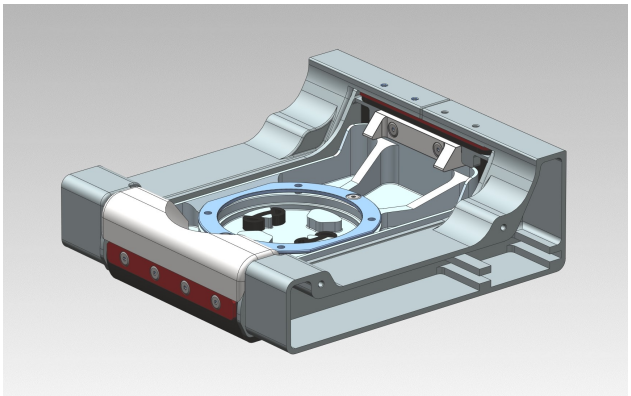

Figure 6.2: Initial design of lateral cases, that should house the sensors and the electronic circuits, attached in a foot sole.

In order to follow the THING project protocols a final design with a cover which makes waterproof the case and allows opening it and working inside has been customized for each foot. In addition, in each case a circular hole has been perforated and covered with a waterproof connector in order to pass a multicore cable from the sensors to the Arduino.

As said before also the box included in the Figure 6.3 has been designed in order to attach the Arduino UNO in the shank. It has enough space to house another board apart from the Arduino if needed and all the wires required inside. It has a hole for the USB connection and another hole has been perforated to pass the multicore cable with all wires coming from the electronic circuits of the sensors.

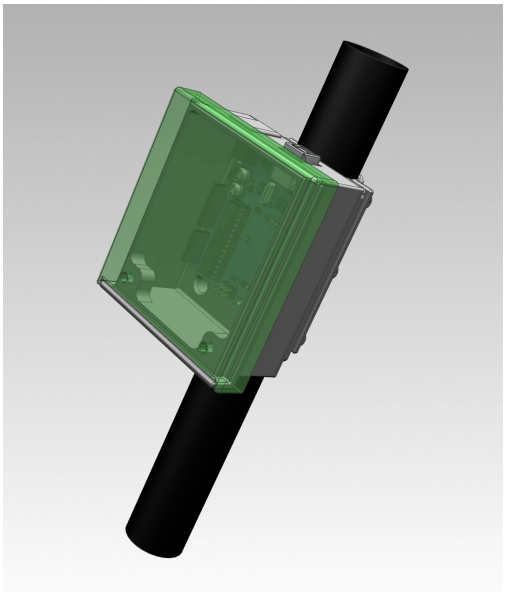

Figure 6.3: Design of the Arduino UNO case attached in the shank.

6.1 Frontal Right Foot - Terrain Analysis Application

The Frontal Right Foot (FRF) integration has been carried out after knowing the results of the foot mockup test. Both piezo vibration sensors and the IMU have been considered to be attached in the FRF of the robot. However, considering the dimensions and the space available in the lateral case for the electronic circuits and the sensors only the IMU was able to fit inside. In order to solve this problem other piezo vibration sensors have been obtained with half the dimensions of the ones used in the foot mockup. So finally the sensors included in the FRF are the ones included in Figure 6.4:

- MiniSense 100H Vibration sensor (Horitzontal)
- MiniSense 100V Vibration sensor (Vertical)
- SparkFun Triple Axis Accelerometer and Gyro Breakout - MPU-6050

(a) 100H Vibration Sensor (b) 100V Vibration Sensor (c) MPU-6050

Figure 6.4: Sensors included in the FRF.

6.1.1 Electronic circuit

The electronic circuit is an adaptation of the circuit used in the foot mockup with the differences of: using different vibration sensors and using capacitors (C_v) of 10µF and operational amplifiers to avoid any kind of interference in the signals. Again the R_c connected in parallel with the piezo is 10MΩ. The IMU is literally connected following its datasheet A.2 and the circuit for the piezo vibration sensors now is the one included in Figure 6.5.

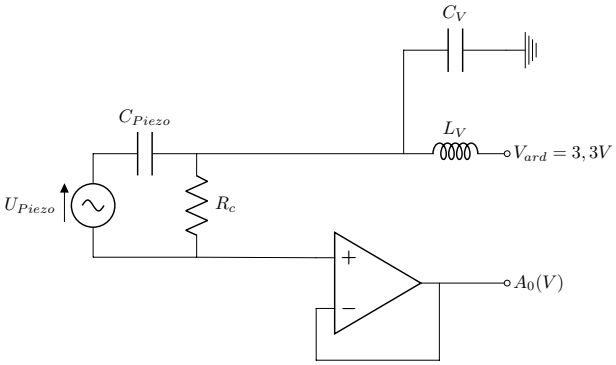

Figure 6.5: Electronic circuit for the Minisense 100H and 100V vibration sensors.

If both 100H and 100V vibration sensors circuits are merged and the IMU is added in the same circuit, the complete circuit for the FRF to perform the terrain analysis is the one included in next Figure 6.6.

6.1.2 Preintegration test

Before integrating the circuit for the 100H and 100V Vibration Sensors and the IMU in the FRF of the ANYmal, a preintegration test has been done in order to see if the new piezo sensors used have the same behavior as the ones used before. The carried out test is similar to the test realized with the foot mockup in the four different surfaces (gravel, rough asphalt, track, smooth flat) in Section 5.3 and the new code used is very similar (Appendix B.2).

The preintegration test contains an experimental part of sliding the ANYmal's foot sole. During the test a similar design to the one presented in Figure 6.2 has been used to house the sensors. The aspect of the foot sole with the lateral cases and the electronic circuits distributed inside is the represented in Figures 6.7 and 6.8; two steel pieces have been added to create a force against the ground; already a hole has been perforated and a multicore cable has been connected between the electronic circuits and the Arduino UNO placed on the top of the steel pieces; the rubber used is from a bike tire which behaves better and has a higher clearance distance than the rubber used in the foot mockup of Section 4.1; and in addition a rope has been tied in order to pull and make the foot sole slide.

The distribution of the piezo vibration sensors with the new components it is different since instead of using four piezo vibration sensors only two are being used and the ones facing to the lateral placed in the foot mockup of Section 5 have been changed for an horizontal one, some pretests showed that the amplitude of the signal obtained with this new configuration was higher meaning it was also better in terms of analyzing it.

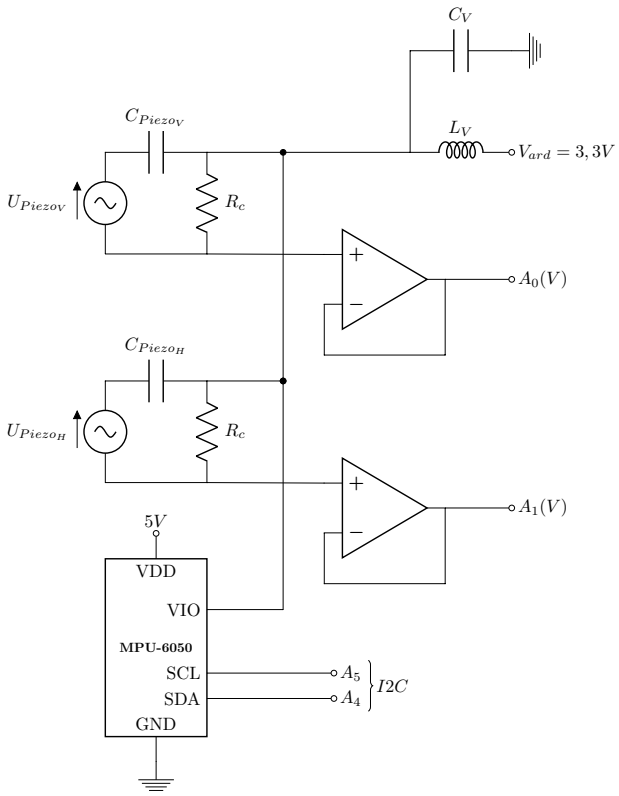

Figure 6.6: FRF electronic circuit. This circuit allows to perform the terrain analysis.

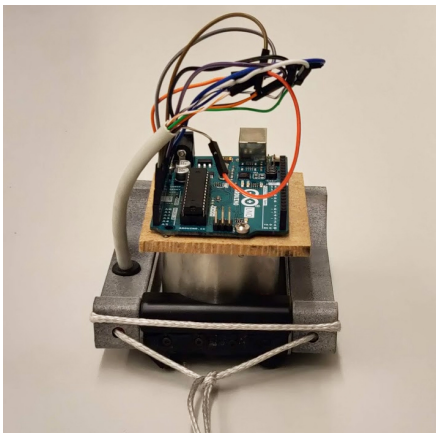

Figure 6.7: Front view of the sole while testing the Mini Sense 100H and 100V Vibration Sensors.

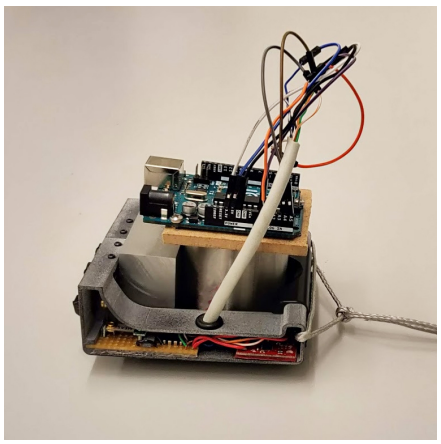

Figure 6.8: Lateral view of the sole while testing the Mini Sense 100H and 100V Vibration Sensors.

In this test the foot sole has been slid twenty times, in each of the four different surfaces (gravel, rough asphalt, track, smooth flat) included in Figure 5.8, during 10 seconds at a constant speed and the data has been saved and analyzed the same way it has been done with the foot mockup test in Section 5.3.

As expected the data obtained with the IMU has the same behavior and the data

obtained with the piezos allows us again to differentiate between surfaces. The results have been summarized, as explained in Section 5.2, again in a Spider Chart included in Figure 6.9 where: V_1 is the voltage of the vertical Vibration sensor; V_2 the voltage of the horizontal Vibration sensor; a_x, a_y, a_z the IMU's acceleration in each of the axis; and ω_x, ω_y, ω_z the IMU's angular velocity in each of the axis. It is possible to see also the new behavior of the 100H and 100V Vibration sensors which is similar to the piezo vibration sensors used in the foot mockup, the main difference probably is that for the horizontal sensors a z-axis vibration create a higher voltage than the one readed in the piezos facing to the y-axis in the foot mockup.

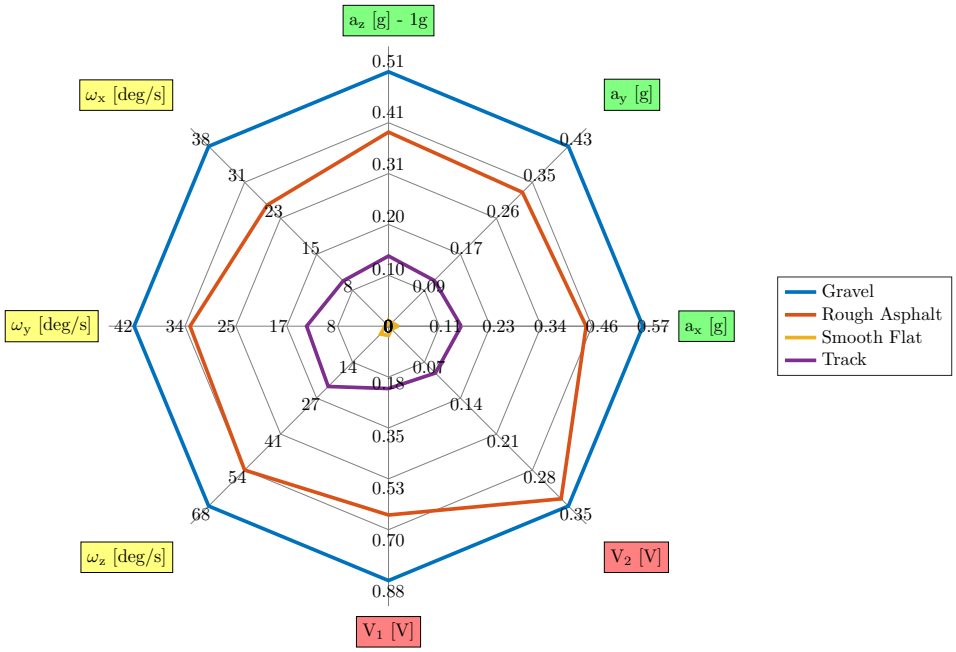

Figure 6.9: Spider chart that contains the results of the analysis done with the parameters measured while sliding the foot sole in the preintegration test.

6.1.3 Vector classification through Machine Learning

In order to verify and check the results obtained with the analysis done the Classification Learner app from the Machine Learning Toolbox of Matlab has been used. The Classification Learner app trains models to classify data, in this project the data includes the measurements done while sliding the foot sole in different surfaces. The purpose of using this tool is to get to know if the analysis done, which ends in the calculation of the standard deviations of every signal, it is valid in order to classify each of the surfaces sampled.

The steps followed while using the Classification Learner have been:

1. **Data preparation**: Using the standard deviations, of each of the parameters measured (voltage from vibration sensors and acceleration and angular velocity from the IMU), calculated, following what's explained in Section 5.2, a matrix has been generated using a vector for each of the columns which includes the eight standard deviations and a number which represent each of the surfaces.

- The standard deviations have been named for the matrix using

$$\sigma^{i}_{j,p} \tag{6.1}$$

  where i represents the surface (1 - Gravel, 2 - Rough Asphalt, 3 - Track, 4 - Smooth Flat), j represents the number of the sample in this surface (repetition, from 1 to 20, in each surface) and the parameter p can be: V_1 for voltage of the vertical Vibration sensor; V_2 for voltage of the horizontal Vibration sensor; a_x, a_y, a_z for the IMU's acceleration in each of the axis; and ω_x, ω_y, ω_z for the IMU's angular velocity in each of the axis.

- The matrix obtained has the following structure:

$$\begin{bmatrix}
\sigma^{1}_{1,a_x} & \dots & \sigma^{1}_{20,a_x} & \sigma^{2}_{1,a_x} & \dots & \sigma^{2}_{20,a_x} & \sigma^{3}_{1,a_x} & \dots & \sigma^{3}_{20,a_x} & \sigma^{4}_{1,a_x} & \dots & \sigma^{4}_{20,a_x} \\
\sigma^{1}_{1,a_y} & \dots & \sigma^{1}_{20,a_y} & \sigma^{2}_{1,a_y} & \dots & \sigma^{2}_{20,a_y} & \sigma^{3}_{1,a_y} & \dots & \sigma^{3}_{20,a_y} & \sigma^{4}_{1,a_y} & \dots & \sigma^{4}_{20,a_y} \\
\sigma^{1}_{1,a_z} & \dots & \sigma^{1}_{20,a_z} & \sigma^{2}_{1,a_z} & \dots & \sigma^{2}_{20,a_z} & \sigma^{3}_{1,a_z} & \dots & \sigma^{3}_{20,a_z} & \sigma^{4}_{1,a_z} & \dots & \sigma^{4}_{20,a_z} \\
\sigma^{1}_{1,\omega_x} & \dots & \sigma^{1}_{20,\omega_x} & \sigma^{2}_{1,\omega_x} & \dots & \sigma^{2}_{20,\omega_x} & \sigma^{3}_{1,\omega_x} & \dots & \sigma^{3}_{20,\omega_x} & \sigma^{4}_{1,\omega_x} & \dots & \sigma^{4}_{20,\omega_x} \\
\sigma^{1}_{1,\omega_y} & \dots & \sigma^{1}_{20,\omega_y} & \sigma^{2}_{1,\omega_y} & \dots & \sigma^{2}_{20,\omega_y} & \sigma^{3}_{1,\omega_y} & \dots & \sigma^{3}_{20,\omega_y} & \sigma^{4}_{1,\omega_y} & \dots & \sigma^{4}_{20,\omega_y} \\
\sigma^{1}_{1,\omega_z} & \dots & \sigma^{1}_{20,\omega_z} & \sigma^{2}_{1,\omega_z} & \dots & \sigma^{2}_{20,\omega_z} & \sigma^{3}_{1,\omega_z} & \dots & \sigma^{3}_{20,\omega_z} & \sigma^{4}_{1,\omega_z} & \dots & \sigma^{4}_{20,\omega_z} \\
\sigma^{1}_{1,V_1} & \dots & \sigma^{1}_{20,V_1} & \sigma^{2}_{1,V_1} & \dots & \sigma^{2}_{20,V_1} & \sigma^{3}_{1,V_1} & \dots & \sigma^{3}_{20,V_1} & \sigma^{4}_{1,V_1} & \dots & \sigma^{4}_{20,V_1} \\
\sigma^{1}_{1,V_2} & \dots & \sigma^{1}_{20,V_2} & \sigma^{2}_{1,V_2} & \dots & \sigma^{2}_{20,V_2} & \sigma^{3}_{1,V_2} & \dots & \sigma^{3}_{20,V_2} & \sigma^{4}_{1,V_2} & \dots & \sigma^{4}_{20,V_2} \\
1 & \dots & 1 & 2 & \dots & 2 & 3 & \dots & 3 & 4 & \dots & 4
\end{bmatrix} \tag{6.2}$$

2. **Training**: After the preparation of the matrix, the training has been performed with a Quadratic Support Vector Machine (SVM) using the last row as response and the first eight rows as the predictors.

3. **Results**: The results have been plotted in a Confussion Matrix (Figure 6.10) where the y-axis contains the True Class or real surface in this case and the x-axis the Predicted Class or predicted surface after the training.

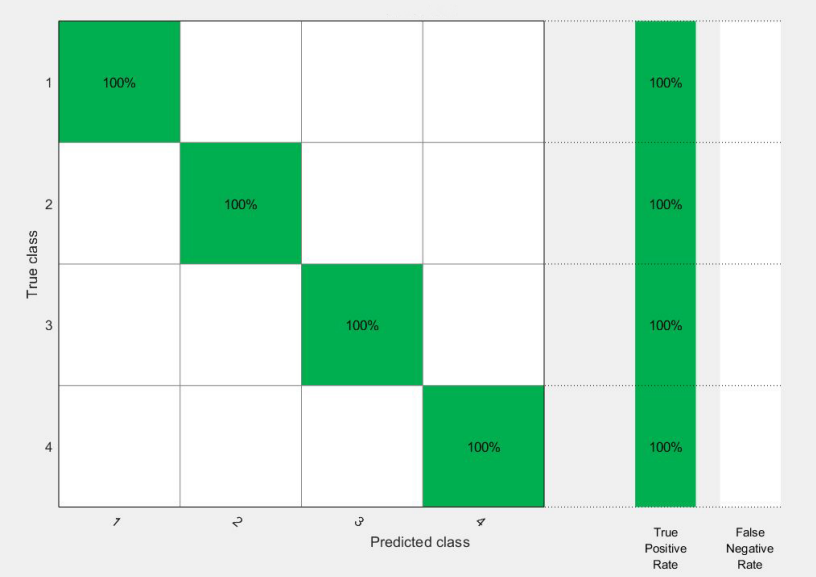

Figure 6.10: Confusion matrix obtained with an SVM training while veryfing the results obtained with the parameters measured while sliding the foot sole. This technique allows to validate the developed application of terrain classification.

Since only four surfaces have been sampled repeatedly, the use of the eight standard deviations calculated for each of the parameters measured in every sample is already valid to perform a terrain classification using this Matlab tool. If a database was generated with hundreds of surfaces probably the use of the time domain signal could not be sufficient and other parameters calculated from the Fast Fourier Transform or the Wavelet Transform could be useful causing the need of higher frequency measurements.

6.1.4 FRF Integration

Already with the electronic circuits decided and the preintegration test giving this satisfactory results the full integration of the right foot has been carried out. Initially a definitive lateral case, shown in a exploded view in Figure 6.11, to house the sensors for the haptic perception has been designed considering the limiting dimensions and its waterproofness.

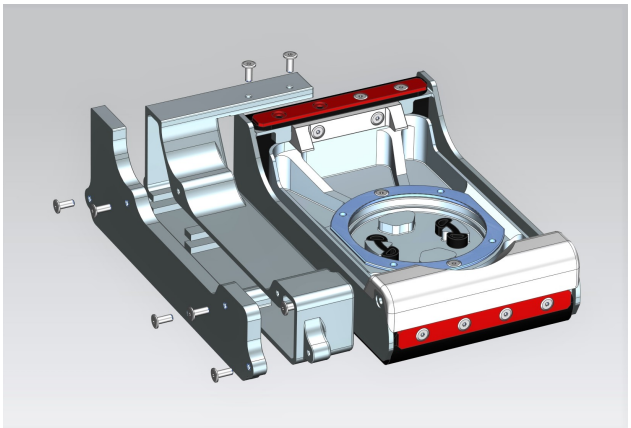

Figure 6.11: Exploded view of the lateral case with its cover and the foot sole.

After 3D printing the case with its cover the integration has been already made, as shown in Figure 6.12, housing the IMU and the Piezo Vibration sensors.

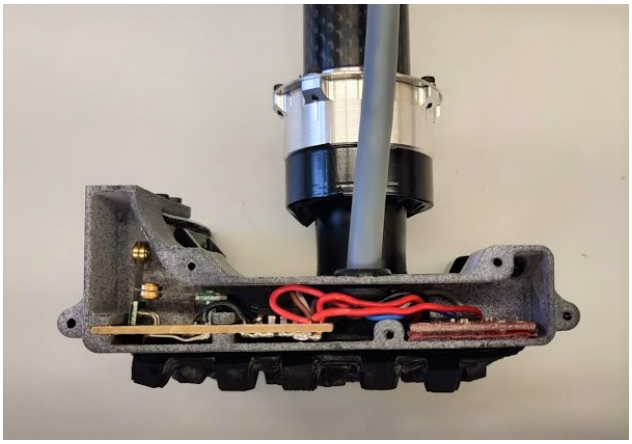

Figure 6.12: Lateral view of the FRF electronic circuits integrated in the lateral case attached in the foot sole.

6.2 Frontal Left Foot - Water Quality Parameters Analysis

The Frontal Left Foot (FLF) has been considered to sense the water quality parameters or to detect metal components. For this purpose a temperature sensor, a pH-meter, a conductivimeter and an inductive sensor were considered. However, after doing some research the decision of not including a pH-meter was done: the dimensions of these sensors exceed the space available and pH-meters also need calibration after each use which makes more difficult the integration. Most of the conductivimeters are also too big and need to be calibrated consequently the decision of building a custom conductivimeter with 2 golden plugs was done.

Finally the components considered for the FLF have been the ones included in Figure 6.13:

- 10K Precision epoxy thermistor - 3950 NTC
- 2 golden plugs for custom conductivimeter
- NAMUR Inductive sensor NF5002

(a) 3950 NTC Thermistor (b) Golden plugs (c) NF5002 Inductive sensor

Figure 6.13: Components included in the foot to analyze water quality properties and to detect metal.

6.2.1 Thermistor circuit

The thermistor selected for this application has been the 10kΩ Precision Epoxy Thermistor - 3950 NTC. Its main characteristics are:

- Diameter 1.3mm.
- Resistance at 25°C: 10kΩ ±1
- Thermistor temperature range: -55°C to 125°C.
- Waterproofness

The circuit used, included in Figure 6.14, is based in the integrated circuit MAX6682 Thermistor-to-Digital Converter (Appendix A.3). The MAX6682 is a sophisticated interface circuit that energizes a low-cost thermistor and converts its temperature-dependent resistance to 10-bit digital data. The MAX6682 powers the thermistor only when a measurement is being made; the power dissipated in the thermistor is minimized.

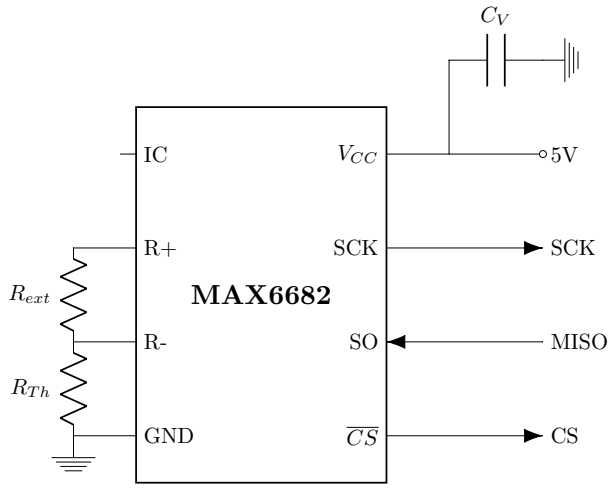

Figure 6.14: MAX6682 typical operation circuit.

Since we are using a NTC 10kΩ thermistor the R_{ext} must be a 7680Ω resistor. The connections SCK, MISO and CS correspond respectively to Arduino 13, 12 and 10 digital I/O. The capacitor C_V, of 10µF, is used to avoid noise in the signal measured.

6.2.2 Conductivimeter

Since normal professional portable conductivimeters, like the one included in Figure 6.15, are too voluminous to be implemented in the small feet we are working with and they need to be calibrated; the idea of using the resistance of the water between two golden plugs has been used. The water properties vary the value of the resistance between two submerged golden plugs separated at a constant distance, this principle is the one used to build a custom conductivimeter.

Figure 6.15: Cole-Parmer Traceable Portable Conductivity Meter with Calibration.

The circuit used to implement a conductivimeter in the foot of the ANYmal is a voltage divider with two resistors: one resistor R_{vd} of 1720Ω in series with the two submerged golden plugs separated 15mm which are the variable resistor in Figure 6.16 and its value depend on the water properties. Again a capacitor C_V, of 10µF, is used to avoid interference in the signal measured.

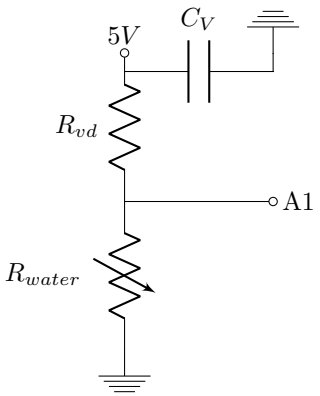

Figure 6.16: Voltage divider circuit used in the built conductivimeter.

In order to separate the golden plugs, a 3D printed piece with two holes has been designed and the plugs have been integrated there, as can be seen in Figure 6.17, to do the calibration at a 15mm distance.

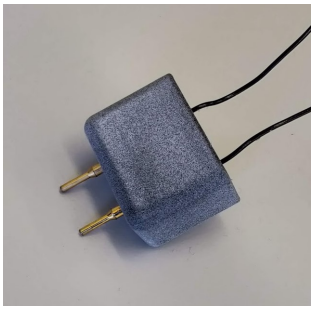

Figure 6.17: Golden plugs installed, with a separation of 15mm, in the designed 3D piece to do the calibration.

In order to calibrate the built conductivimeter an experiment with pure water and salt (NaCl) has been done at a temperature of 22^{o}C (the maximum mean temperature found in the Zurich's sewer) considering that higher temperatures mean higher conductivity. Using the low-calibrated portable conductivimeter from Pancellent included in Figure 6.18 for conductivity values below 2500μS/cm and a salinity to conductivity conversion for values of conductivity over 2500μS/cm [13], the experiment consisted in slowly adding salt to a volume of 500ml of pure water to find a correlation to follow with the built condutivimeter.

Figure 6.18: Pancellent low-calibrated portable conductivimeter.

The next Table 6.1 sums up the different values of EC of the salty water and the voltage read in the Arduino analog input.

	Salinity (g/l)	**Voltage (V)**	**Conductivity (μS/cm)**
Low conductivity calibrated conductivimeter	-	4,6188	61
	-	2,8886	383
	-	2,4585	661
	-	2,2385	1070
	-	2,0283	1780
	-	1,9550	2090
Salinity - Conductivity conversion	2	1,7400	3650
	4	1,5445	6900
	6	1,4907	10100
	8	1,4125	13200
	10	1,3881	16200

Table 6.1: Results obtained in the experiment performed to calibrate the built conductivimeter. These results have been used to obtain a relationship between voltage and EC afterwards.

In order to get a relationship between Voltage and EC the results have been plotted and two equations between two different ranges have been selected as the ones relating voltage and conductivity using this custom conductivimeter. Everything it is represented in the Figure 6.19.

The following piecewise equation (Equation 6.3) is the one used to do the Voltage to EC conversion:

$$a_1 = 11425,3080157630$$

$$a_2 = -179931,426257226$$

$$a_3 = 1149265,81336814$$

$$a_4 = -3829540,65688212$$

$$a_5 = 7049406,23704861$$

$$a_6 = -6823273,21685527$$

$$a_7 = 2725517,70005086$$

$$b_1 = -3,89162612689167$$

$$b_2 = 23431.86649233335$$

$$EC[\mu S/cm] = \begin{cases} a_1V^6 + a_2V^5 + a_3V^4 + a_4V^3 + a_5V^2 + a_6V + a_7, & \text{if } 1.4 < V[V] < 2.4 \\ b_2V^{b_1}, & \text{if } 2.4 \leq V[V] < 4.4 \end{cases} \tag{6.3}$$

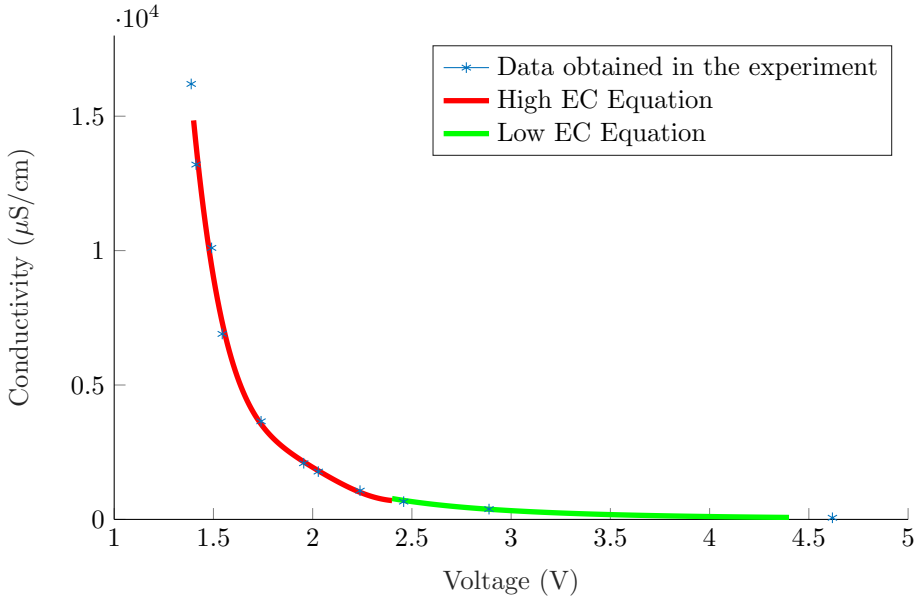

Figure 6.19: Graph that includes the data from the experiment performed to calibrate the custom conductivimeter and the two different equations, of the piecewise equation 6.3, in their corresponding range, used to convert the voltage obtained from the Arduino input to EC.

Using this relation between voltage and EC we are not obtaining a high resolution conductivimeter. However, the range of EC normally found, in the Zurich's sewer, between 600μS/cm to 800μS/cm can be measured accurately enough with the custom conductivimeter; and the minimum value considered as dangerous EC value for the sewer, which it depends on the country and it is around 2000μS/cm, can be also found in the range where the equations have been validated. If the conductivity is too high (over 20000μS/cm) the voltage will be lower than 1.4V and if the water is pure the conductivity would be around 0μS/cm and the voltage near 5V.

6.2.3 Inductive sensor

The last sensor considered to be integrated in the left foot is the inductive sensor NAMUR NF5002, which is a small IP67 inductive sensor with only two wires. It has the capacity to detect metal in a 2mm range. The length of its cable can be adapted for the integration as can be seen in Figure 6.20 were the whole cable has been cut and only 5cm of the two wires inside the cables are left.

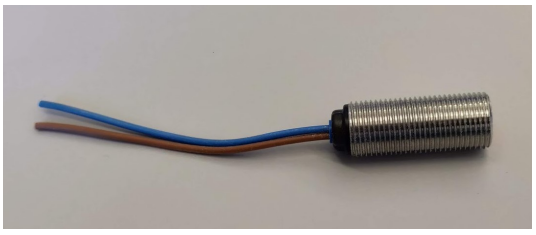

Figure 6.20: NAMUR NF5002 inductive sensor.

The circuit used is the one included in next Figure 6.21. Basically it works this way: in presence of metal a very low current it is allowed to pass through the inductive sensor and the Arduino analog input, located between the $1k\Omega$ resistor (R_i) and the inductive sensor, reads a low signal voltage; when there is no presence of a metal component a high voltage signal is read in the Arduino analog input because the inductive sensor induces a current through it.

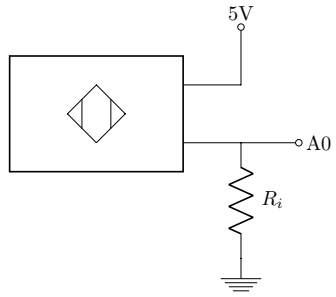

Figure 6.21: Circuit for the NF5002 2-wires inductive sensor.

6.2.4 FLF integration

The whole circuit of the FLF (thermistor, custom conductivimeter and inductive sensor) is the one included in Figure 6.22. All circuit have in common the ground and the circuit from the thermistor and the inductive sensor are fed with the same Arduino output at 5V. The 5V voltage, thats feeds the conductivimeter, needs to be isolated from the rest of the circuits. This way only 8 wires (an 8-core cable) are needed to implement the connections from the electronic circuits of the sensors to the Arduino.

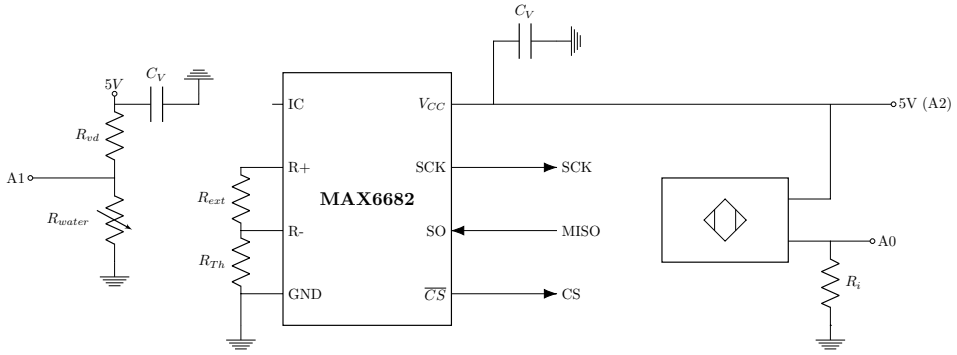

Figure 6.22: FLF electronic circuits.

Once the circuit was designed and implemented in a board, a final design for the FLF lateral case has been developed to house all the components, considering the initial design in Figure 6.2. This final design is included in the exploded view of Figure 6.23. It is a waterproof case where the two golden plugs and the termistor are in a compartment that can be submerged in the water and the inductive sensor is facing forward in order to check the composition of the explored objects looking for metal. The dimensions of the lateral case are surpassing by a few millimeters the ones expected; this problem appears when including all the sensors and because the custom conductivimeter that needs at least 15mm between plugs to be considered as accurate while measuring the EC of the water.

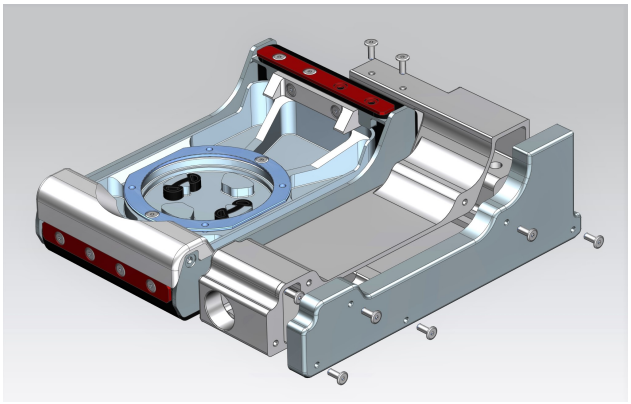

Figure 6.23: Exploded view of the left lateral case with its cover and the foot sole.

After 3D printing the lateral case, the integration with the sensors is the one included in next Figure 6.24.

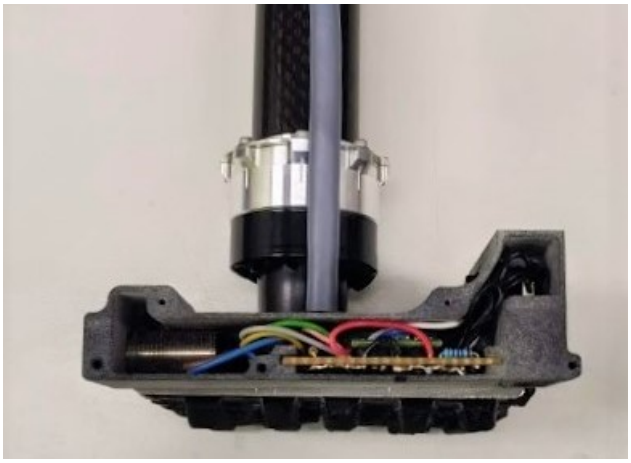

Figure 6.24: Lateral view of the FLF electronic circuits integrated in the lateral case attached in the foot sole.

6.3 Prototype - Final integration

The prototype built consists in the integration developed, in last sections 6.1 and 6.2, in both of the frontal shanks and feet of the ANYmal. This final integration is included in Figure 6.25, where: both lateral cases used to house the sensors have been covered and attached next to the correspondent feet sole; the Arduino cases have been attached in the shanks; and the connections between the electronic circuits and Arduinos have been done (Appendix C).

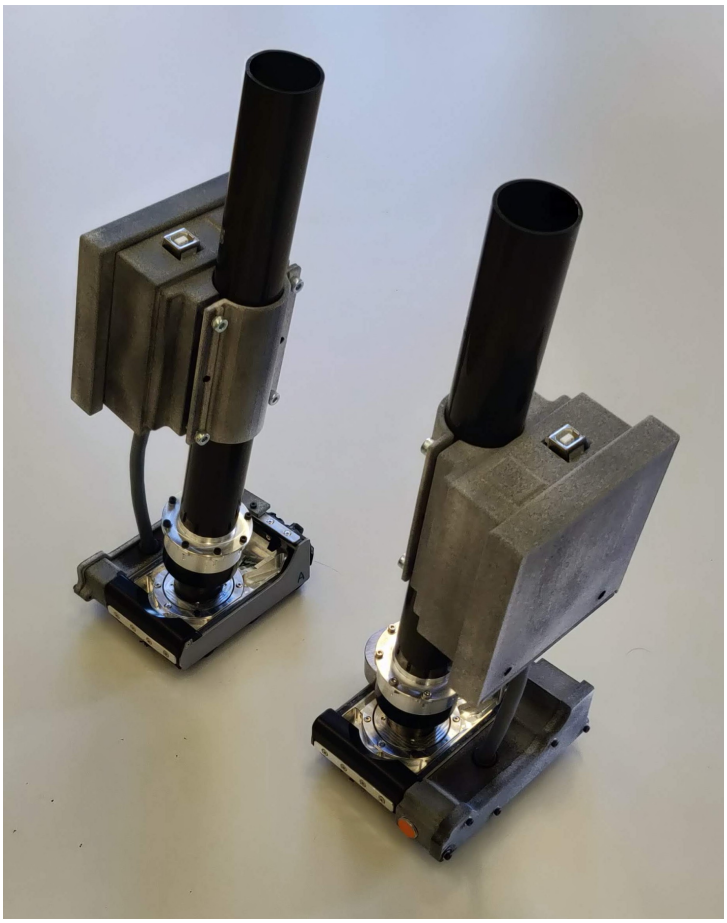

Figure 6.25: Prototype for the THING project. It includes the integration of sensors for an advanced haptic perception and to perform water quality analysis.

The integration done in both of the frontal feet has had also the objective of maintaining the symmetry, as much as possible, in the ANYmal's body.

Chapter 7

Test with the ANYmal

Once the integration has been carried out in both frontal shanks and feet, these have been attached in the ANYmal, as can be seen in Figure 7.1, to perform an initial test of the developed applications.

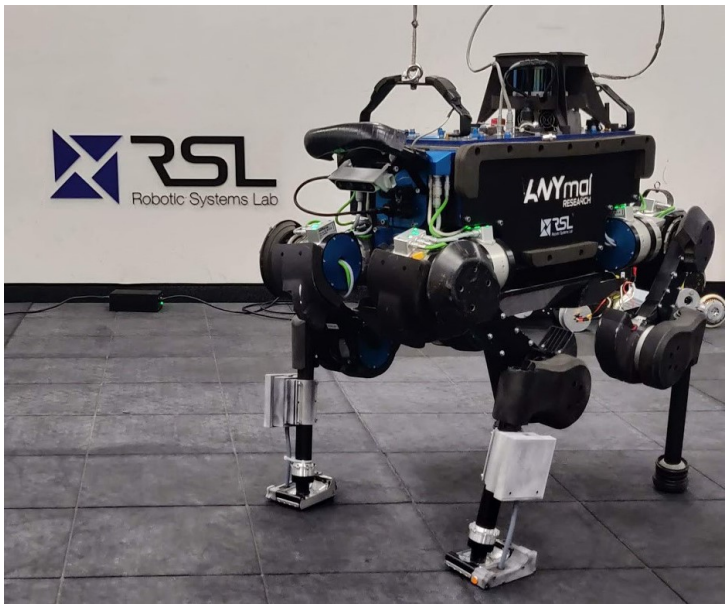

Figure 7.1: The ANYmal standing in the RSL with the prototype installed in both frontal feet developed within the THING project.

The purpose of this initial test was to see if the prototype built allows the ANYmal walking and performing a scratching motion in different surfaces. After seeing that it was capable of walking, a scratching motion was prepared and performed on three different surfaces (Figure 7.2): the rubber of the RSL ground, smooth wood and plastic grass.

The scratching motion was performed in all the surfaces with any problem. But, the behaviour of the passive ankle was not the one expected because the movement of the feet was not performed with a torque control motion. The normal forces the feet were receiving from the ground should be considered to perform this scratching motion.

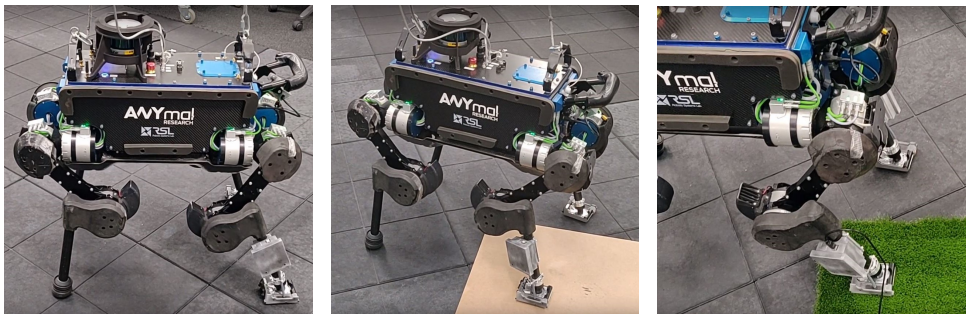

(a) Rubber (b) Wood (c) Plastic grass

Figure 7.2: The ANYmal standing in all different surfaces where the scratching motion was tested.

With this test also appeared another point to consider. If the foot of the robot was pressing to much against the surface, it could get stuck if the friction coefficient of the surface was high enough. This problem was appearing when performing the scratching motion on the rubber.

Even though samples were taken with the Arduino UNO, attached in the frontal right foot, capable of performing a haptic perception, the results from this samples were not considered to verify the new haptic perception included in the ANYmal because the scratching motion should be adapted before.

Chapter 8

Conclusions

This project contributes with the goals of the THING project of performing inspections in challenging environments. Several improvements for the ANYmal have been developed following these goals. On the one hand, a tool that improves the capacities of the robot towards advanced perception in the environment has been developed; on the other hand, a prototype capable of performing sewer inspections has been built.

The main purpose of the project was the development of sensorized feet to perform sewer inspections. Although the goals of the project were challenging, the integration of sensors attached in the frontal feet of the ANYmal has been carried out.

First, data has been obtained while testing the selected sensors (vibrations sensors and IMU) to develop a haptic perception. These tests have allowed us to determine that with the use of these sensors we can differentiate between surfaces just by scratching the feet of the ANYmal on them. These promising results have allowed us to move forward into installing these sensors in a case attached in a foot sole of the ANYmal.

Moreover, a second case containing a thermistor, a conductivimeter and an inductive sensor has been attached to a second foot sole to perform water quality analysis or detect metal in the field.

Returning to the haptic perception, the results obtained have also been verified with the Classification Learner app of the Machine Learning Toolbox of Matlab.

To finish the project, the prototype (cases housing sensors attached in the ANYmal's feet) has been installed in the ANYmal and a test has been performed demonstrating that the use of these built cases does not affect the robot's mobility. However, the objective of this test was to prove the new haptic perception developed during the project. As for this, the results have not been the desired because the scratching motion used was not developed using torque control. While performing the scratching motion, the foot should always apply the same controlled force against the ground.

However, the built prototype gives the ANYmal the opportunity of performing autonomous sewer inspections. This could avoid the need of introducing sewer's operators in the harsh environment that the sewage system is for humans. Furthermore, the advanced perception developed for the recognition or

differentiation between surfaces open the ANYmal many doors to other fields such as soil texture analysis or road flaws inspections.

8.1 Future work

Before improving the sensors integration in the ANYmal, a new test using a torque control scratching motion should be performed. This would allow us to check the developed application with the prototype installed in the ANYmal.

If the results were promising, smaller electronics components and customized boards could be used. Moreover, the connections between components could be achieved using less space and the full waterproofness of all the components should be resolved.

In a short term, the prototype will be tested in the sewer for the THING project. For this test, the cases attached in the feet of the robot should be sealed with silicon or hot glue.

Besides, in order to accomplish the terrain classification using tools like Classification Learner of Matlab, a database with samples measured in all different kind of surfaces the robot could find in these inspections should be created. This way, a tool could be defined to differentiate any possible terrain the robot could work in.

From the beginning, the addition of pressure force sensors was also considered. The idea was to use these sensors, installed in the foot soles of the ANYmal, to get to know which parts of the sole were touching the ground and how the weight of the robot was distributed in the support points (feet). The integration of these sensors would also allow the improvement of the developed haptic perception. However, dealing with this concept was not possible because the RSL engineers were working in parallel with the foot sole.

Now that the design of the foot soles has been defined, the addition of these pressure force sensors could be a concept in which further research could be done and an adapted sole could be designed with the purpose of improving towards to even more advanced perception.

Bibliography

[1] "subTerranean Haptic INvestiGator / Projects / H2020 / CORDIS / European Commission," https://cordis.europa.eu/project/rcn/213179_en.html, accessed: 2018-05-25.

[2] M. Hutter, C. Gehring, D. Jud, A. Lauber, C. D. Bellicoso, V. Tsounis, J. Hwangbo, K. Bodie, P. Fankhauser, M. Bloesch, R. Diethelm, S. Bachmann, A. Melzer, and M. Hoepflinger, "ANYmal - a highly mobile and dynamic quadrupedal robot," in *2016 IEEE/RSJ International Conference on Intelligent Robots and Systems (IROS)*, Oct 2016, pp. 38–44.

[3] M. Hutter, K.Roman, H.Kolvenbach, L.Paez, and L. Klajd, "Towards a passive adaptive planar foot with ground orientation and contact force sensing for legged robots," in *2018 IEEE/RSJ International Conference on Intelligent Robots and Systems (IROS)*, Oct 2018.

[4] "SOLO / RedZone Robotics, Wastewater Management," https://www.redzone.com/technology/solo, accessed: 2018-06-10.

[5] "ARSI - Aereal Robot for Sewer Inspection," https://eurecat.org/en/portfolio-items/aerial-robot-for-sewer-inspection/, accessed: 2018-06-10.

[6] "SIAR - Sewer Inspection Autonomous Robot - The European Coordination Hub for Open Robotics Development," http://echord.eu/essential_grid/siar/, accessed: 2018-06-11.

[7] N. Elkmann, S. Kutzner, J. Saenz, B. Reimann, F. Schultke, and H. Althoff, "Fully automatic inspection systems for large underground concrete pipes partially filled with wastewater," in *2006 IEEE/RSJ International Conference on Intelligent Robots and Systems*, Oct 2006, pp. 4234–4238.

[8] *Parameters of Water Quality: Interpretation and Standards.* Environmental Protection Agency (EPA), February 2001.

[9] "SCiO - The World's First Pocket Sized Molecular Sensor," https://www.consumerphysics.com/, accessed: 2018-06-19.

[10] P.Dallaire, P. Giguère, D. Émond, and B. Chaib-Draa, "Autonomous tactile perception: A combined improved sensing and bayesian nonparametric approach," *Robot. Auton. Syst.*, vol. 62, no. 4, pp. 422–435, April 2014.

[11] M. A. Hoepflinger, C. D. Remy, M. Hutter, L. Spinello, and R. Siegwart, "Haptic terrain classification for legged robots," in *2010 IEEE International Conference on Robotics and Automation*, May 2010, pp. 2828–2833.

[12] "CoolTerm," https://coolterm.en.lo4d.com/details, accessed: 2018-06-30.

[13] P. K. Weyl, "On the change in electrical conductance of seawater with temperature 1," *Limnology and Oceanography*, vol. 9, no. 1, pp. 75–78, 2003.

[14] C. Scrimgeour, "Soil sampling and methods of analysis (second edition). edited by m. r. carter and e. g. gregorich. boca raton, fl, usa," vol. 44, July 2008.

[15] D. A Horneck, D. Sullivan, J. Owen Jr, and J. M Hart, "Soil test interpretation guide," July 2011.

Appendix A

Datasheets

A.1 Piezo Vibration Sensor datasheet

LDT with Crimps Vibration Sensor/Switch

measurement SPECIALTIES

- Piezo Film Sensors
- High Sensativity
- AC Coupled
- Laminated
- Robust

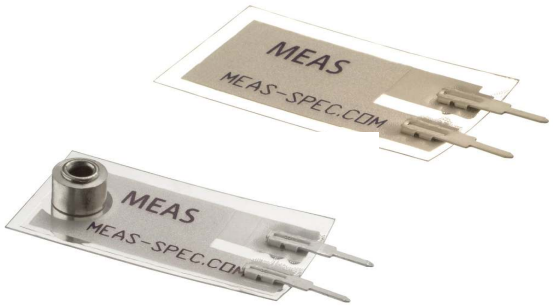

The LDT0-028K is a flexible component comprising a 28 µm thick piezoelectric PVDF polymer film with screen-printed Ag-ink electrodes, laminated to a 0.125 mm polyester substrate, and fitted with two crimped contacts. As the piezo film is displaced from the mechanical neutral axis, bending creates very high strain within the piezopolymer and therefore high voltages are generated. When the assembly is deflected by direct contact, the device acts as a flexible "switch", and the generated output is sufficient to trigger MOSFET or CMOS stages directly. If the assembly is supported by its contacts and left to vibrate "in free space" (with the inertia of the clamped/free beam creating bending stress), the device will behave as an accelerometer or vibration sensor. Adding mass, or altering the free length of the element by clamping, can change the resonant frequency and sensitivity of the sensor to suit specific applications. Multi-axis response can be achieved by positioning the mass off center. The LDTM-028K is a vibration sensor where the sensing element comprises a cantilever beam loaded by an additional mass to offer high sensitivity at low frequencies.

dimensions

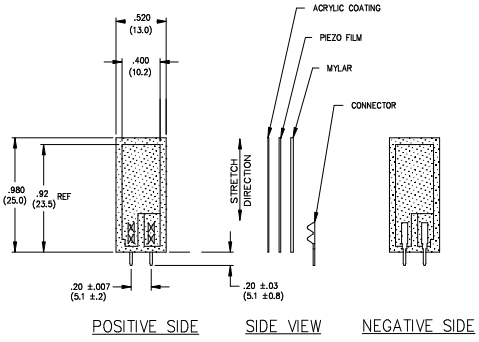

FEATURES

- Solder Tab Connection
- Both No Mass & With Mass Version
- Withstands High Impact
- Operating Temperature: 0ºC to 85ºC
- Storage Temperature: -40ºC to 85 ºC
- Higher Temperature Version up to 125 ºC available on a Custom Basis

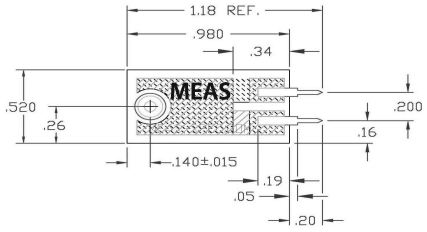

APPLICATIONS

- Vibration Sensing in Washing Machine
- Low Power Wakeup Switch
- Low Cost Vibration Sensing
- Car Alarms
- Body Movement
- Security Systems

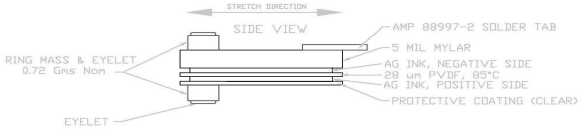

LDT with Crimps Vibration Sensor/Switch

measurement SPECIALTIES

examples of properties

Four different experiments serve to illustrate the various properties of this simple but versatile component.

Experiment #1
LDT0 as Vibration Sensor - with the crimped contacts pushed through a printed-circuit board, the LDT0 was soldered carefully in place to anchor the sensor. A charge amplifier was used to detect the output signal as vibration from a shaker table was applied (using a charge amplifier allows a very long measurement time constant and thus allows the "open-circuit" voltage response to be calculated). Small masses (approximately 0.26g increments) were then added to the tip of the sensor, and the measurement repeated. Results are shown in Table 1 and the overlaid plots in Fig. 1. Without adding mass, the LDT0 shows a resonance around 180 Hz. Adding mass to the tip reduces the resonance frequency and increases "baseline" sensitivity.

LDT0 Sensitivity: Effect of Added Mass
(Figure 1)

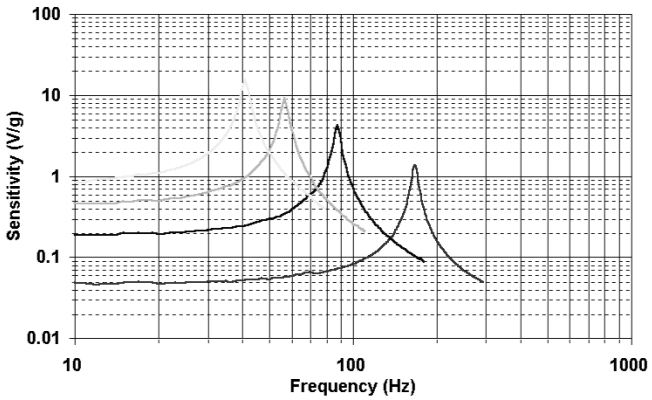

TABLE 1: LDT0 as Vibration Sensor (see Fig 1)

Added Mass	Baseline Sensitivity	Sensitivity at Resonance	Resonant Frequency	+3 Db Frequency
0	50 mV/g	1.4 V/g	180 Hz	90 Hz
1	200 mV/g	4 V/g	90 Hz	45 Hz
2	400 mV/g	8 V/g	60 Hz	30 Hz
3	800 mV/g	16 V/g	40 Hz	20 Hz

Experiment #2
LDT0 as Flexible Switch - using a charge amplifier to obtain "open-circuit" voltage sensitivity, the output was measured for controlled tip deflections applied to the sensor (supported by its crimped contacts as described above). 2 mm deflection was sufficient to generate about 7 V. Voltages above 70V could be generated by bending the tip of the sensor through 90° (see Table 2, Fig. 2).

LDT0: Voltage Output vs Tip deflection
(Figure 2)

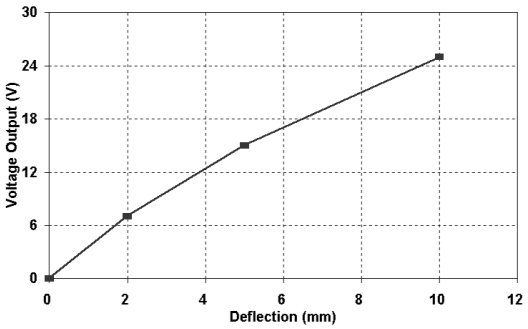

LDT with Crimps Vibration Sensor/Switch

measurement SPECIALTIES

examples of Properties (continued)

TABLE 2: LDT0 as Flexible Switch (see Fig 2)

Tip Deflection	Charge Output	o/c Voltage Output
2 mm	3.4 nC	7 V
5 mm	7.2 nC	15 V
10 mm	10 - 12 nC	20 - 25 V
max (90E)	> 30 nC	> 70 V

Experiment #3
LDT0 Electrical Frequency Response - when the source capacitance of around 480 pF is connected to a resistive input load, a high-pass filter characteristic results. Using an electronic noise source to generate broad-band signals, the effect of various load resistances was measured and the -3 dB point of the R-C filter determined (see Table 3, Fig. 3).

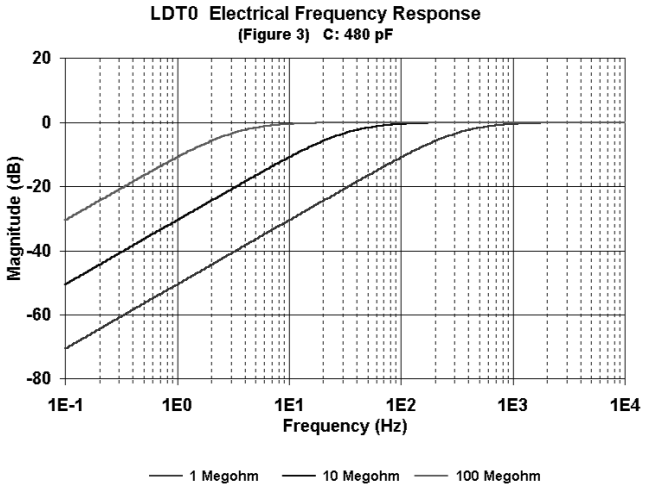

TABLE 3: LDT0 Electrical Frequency Response
(see Fig 3)
(480 pF source capacitance)

Load Resistance	-3 db Frequency
1 Megohm	330 Hz
10 Megohm	33 Hz
100 Megohm	3.3 Hz

LDT with Crimps Vibration Sensor/Switch

Experiment #4
LDT0 Clamped at Different Lengths - using simple clamping fixture, the vibration sensitivity was measured (as in (1) above) as the clamp was moved to allow different "free" lengths to vibrate. The sensor may be "tuned" to suit specific frequency response requirements (see Table 4, Fig. 4).

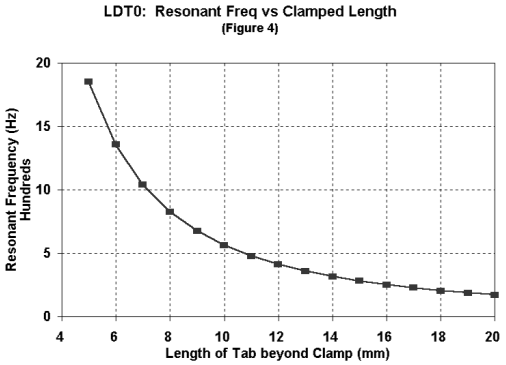

TABLE 4: LDT0 Clamped at Different Lengths (See Fig. 4)

Length Beyond Clamp	Resonant Frequency	Settling Time (5 cyc)
20 mm (no clamp)	180 Hz	28 msec
16 mm	250 Hz	20 msec
11 mm	500 Hz	10 msec
7 mm	1000 Hz	5 msec

ordering information

Description	Part Number
LDT0-028K	1002794-0
LDTM-028K	1005447-1

North America

Measurement Specialties, Inc.
1000 Lucas Way
Hampton, VA 23666
Sales and Customer Service
Tel: +1-800-745-8008 or
+1-757-766-1500
Fax: +1-757-766-4297
Technical Support
Email: piezo@meas-spec.com

Europe

MEAS Deutschland GmbH
Hauert 13
44227 Dortmund
Germany
Sales and Customer Service
Tel: +49 (0)231 9740 21
Technical Support
Tel: +49 (0)6074 862822
Email: piezoeurope@meas-spec.com

Asia

Measurement Specialties (China), Ltd.
No. 26 Langshan Road
Shenzhen High-Tech Park (North)
Nanshan District
Shenzhen, China 518107
Sales and Customer Service
Tel: +86 755 3330 5088
Technical Support
Email: piezo@meas-spec.com

A.2 MPU-6050 datasheet

6 Electrical Characteristics

6.1 Gyroscope Specifications

VDD = 2.375V-3.46V, VLOGIC (MPU-6050 only) = 1.8V±5% or VDD, T_A = 25°C

PARAMETER	CONDITIONS	MIN	TYP	MAX	UNITS	NOTES
GYROSCOPE SENSITIVITY						
Full-Scale Range	FS_SEL=0		±250		º/s	
	FS_SEL=1		±500		º/s	
	FS_SEL=2		±1000		º/s	
	FS_SEL=3		±2000		º/s	
Gyroscope ADC Word Length			16		bits	
Sensitivity Scale Factor	FS_SEL=0		131		LSB/(º/s)	
	FS_SEL=1		65.5		LSB/(º/s)	
	FS_SEL=2		32.8		LSB/(º/s)	
	FS_SEL=3		16.4		LSB/(º/s)	
Sensitivity Scale Factor Tolerance	25°C	-3		+3	%	
Sensitivity Scale Factor Variation Over Temperature			±2		%	
Nonlinearity	Best fit straight line; 25°C		0.2		%	
Cross-Axis Sensitivity			±2		%	
GYROSCOPE ZERO-RATE OUTPUT (ZRO)						
Initial ZRO Tolerance	25°C		±20		º/s	
ZRO Variation Over Temperature	-40°C to +85°C		±20		º/s	
Power-Supply Sensitivity (1-10Hz)	Sine wave, 100mVpp; VDD=2.5V		0.2		º/s	
Power-Supply Sensitivity (10 - 250Hz)	Sine wave, 100mVpp; VDD=2.5V		0.2		º/s	
Power-Supply Sensitivity (250Hz - 100kHz)	Sine wave, 100mVpp; VDD=2.5V		4		º/s	
Linear Acceleration Sensitivity	Static		0.1		º/s/*g*	
SELF-TEST RESPONSE						
Relative	Change from factory trim	-14		14	%	1
GYROSCOPE NOISE PERFORMANCE	**FS_SEL=0**					
Total RMS Noise	DLPFCFG=2 (100Hz)		0.05		º/s-rms	
Low-frequency RMS noise	Bandwidth 1Hz to10Hz		0.033		º/s-rms	
Rate Noise Spectral Density	At 10Hz		0.005		º/s/ √ Hz	
GYROSCOPE MECHANICAL FREQUENCIES						
X-Axis		30	33	36	kHz	
Y-Axis		27	30	33	kHz	
Z-Axis		24	27	30	kHz	
LOW PASS FILTER RESPONSE						
	Programmable Range	5		256	Hz	
OUTPUT DATA RATE						
	Programmable	4		8,000	Hz	
GYROSCOPE START-UP TIME	**DLPFCFG=0**					
ZRO Settling (from power-on)	to ±1º/s of Final		30		ms	

1. Please refer to the following document for further information on Self-Test: *MPU-6000/MPU-6050 Register Map and Descriptions*

6.2 Accelerometer Specifications

VDD = 2.375V-3.46V, VLOGIC (MPU-6050 only) = 1.8V±5% or VDD, T_A = 25°C

PARAMETER	CONDITIONS	MIN	TYP	MAX	UNITS	NOTES
ACCELEROMETER SENSITIVITY						
Full-Scale Range	AFS_SEL=0		±2		*g*	
	AFS_SEL=1		±4		*g*	
	AFS_SEL=2		±8		*g*	
	AFS_SEL=3		±16		*g*	
ADC Word Length	Output in two's complement format		16		bits	
Sensitivity Scale Factor	AFS_SEL=0		16,384		LSB/*g*	
	AFS_SEL=1		8,192		LSB/*g*	
	AFS_SEL=2		4,096		LSB/*g*	
	AFS_SEL=3		2,048		LSB/*g*	
Initial Calibration Tolerance			±3		%	
Sensitivity Change vs. Temperature	AFS_SEL=0, -40°C to +85°C		±0.02		%/°C	
Nonlinearity	Best Fit Straight Line		0.5		%	
Cross-Axis Sensitivity			±2		%	
ZERO-G OUTPUT						
Initial Calibration Tolerance	X and Y axes		±50		m*g*	1
	Z axis		±80		m*g*	
Zero-G Level Change vs. Temperature	X and Y axes, 0°C to +70°C		±35			
	Z axis, 0°C to +70°C		±60		m*g*	
SELF TEST RESPONSE						
Relative	Change from factory trim	-14		14	%	2
NOISE PERFORMANCE						
Power Spectral Density	@10Hz, AFS_SEL=0 & ODR=1kHz		400		μ*g*/√Hz	
LOW PASS FILTER RESPONSE						
	Programmable Range	5		260	Hz	
OUTPUT DATA RATE						
	Programmable Range	4		1,000	Hz	
INTELLIGENCE FUNCTION INCREMENT			32		mg/LSB	

1. Typical zero-g initial calibration tolerance value after MSL3 preconditioning
2. Please refer to the following document for further information on Self-Test: *MPU-6000/MPU-6050 Register Map and Descriptions*

6.3 Electrical and Other Common Specifications

VDD = 2.375V-3.46V, VLOGIC (MPU-6050 only) = 1.8V±5% or VDD, T_A = 25°C

PARAMETER	CONDITIONS	MIN	TYP	MAX	Units	Notes
TEMPERATURE SENSOR						
Range			-40 to +85		°C	
Sensitivity	Untrimmed		340		LSB/ºC	
Temperature Offset	35°C		-521		LSB	
Linearity	Best fit straight line (-40°C to +85°C)		±1		°C	
VDD POWER SUPPLY						
Operating Voltages		2.375		3.46	V	
Normal Operating Current	Gyroscope + Accelerometer + DMP		3.9		mA	
	Gyroscope + Accelerometer (DMP disabled)		3.8		mA	
	Gyroscope + DMP (Accelerometer disabled)		3.7		mA	
	Gyroscope only (DMP & Accelerometer disabled)		3.6		mA	
	Accelerometer only (DMP & Gyroscope disabled)		500		µA	
Accelerometer Low Power Mode Current	1.25 Hz update rate		10		µA	
	5 Hz update rate		20		µA	
	20 Hz update rate		70		µA	
	40 Hz update rate		140		µA	
Full-Chip Idle Mode Supply Current			5		µA	
Power Supply Ramp Rate	Monotonic ramp. Ramp rate is 10% to 90% of the final value			100	ms	
VLOGIC REFERENCE VOLTAGE	MPU-6050 only					
Voltage Range	VLOGIC must be ≤VDD at all times	1.71		VDD	V	
Power Supply Ramp Rate	Monotonic ramp. Ramp rate is 10% to 90% of the final value			3	ms	
Normal Operating Current			100		µA	
TEMPERATURE RANGE						
Specified Temperature Range	Performance parameters are not applicable beyond Specified Temperature Range	-40		+85	°C	

6.4 Electrical Specifications, Continued

VDD = 2.375V-3.46V, VLOGIC (MPU-6050 only) = 1.8V±5% or VDD, T_A = 25°C

PARAMETER	CONDITIONS	MIN	TYP	MAX	Units	Notes
SERIAL INTERFACE						
SPI Operating Frequency, All Registers Read/Write	MPU-6000 only, Low Speed Characterization		100 ±10%		kHz	
	MPU-6000 only, High Speed Characterization		1 ±10%		MHz	
SPI Operating Frequency, Sensor and Interrupt Registers Read Only	MPU-6000 only		20 ±10%		MHz	
I^2C Operating Frequency	All registers, Fast-mode			400	kHz	
	All registers, Standard-mode			100	kHz	
I^2C ADDRESS	AD0 = 0		1101000			
	AD0 = 1		1101001			
DIGITAL INPUTS (SDI/SDA, AD0, SCLK/SCL, FSYNC, /CS, CLKIN)						
V_{IH}, High Level Input Voltage	MPU-6000	0.7*VDD			V	
	MPU-6050	0.7*VLOGIC			V	
V_{IL}, Low Level Input Voltage	MPU-6000			0.3*VDD	V	
	MPU-6050			0.3*VLOGIC	V	
C_i, Input Capacitance			< 5		pF	
DIGITAL OUTPUT (SDO, INT)						
V_{OH}, High Level Output Voltage	R_{LOAD}=1MΩ; MPU-6000	0.9*VDD			V	
	R_{LOAD}=1MΩ; MPU-6050	0.9*VLOGIC			V	
V_{OL1}, LOW-Level Output Voltage	R_{LOAD}=1MΩ; MPU-6000			0.1*VDD	V	
	R_{LOAD}=1MΩ; MPU-6050			0.1*VLOGIC	V	
$V_{OL.INT1}$, INT Low-Level Output Voltage	OPEN=1, 0.3mA sink Current			0.1	V	
Output Leakage Current	OPEN=1		100		nA	
t_{INT}, INT Pulse Width	LATCH_INT_EN=0		50		µs	

6.5 Electrical Specifications, Continued

Typical Operating Circuit of Section 7.2, VDD = 2.375V-3.46V, VLOGIC (MPU-6050 only) = 1.8V±5% or VDD, T_A = 25°C

Parameters	Conditions	Typical	Units	Notes
Primary I^2C I/O (SCL, SDA)				
V_{IL}, LOW-Level Input Voltage	MPU-6000	-0.5 to 0.3*VDD	V	
V_{IH}, HIGH-Level Input Voltage	MPU-6000	0.7*VDD to VDD + 0.5V	V	
V_{hys}, Hysteresis	MPU-6000	0.1*VDD	V	
VIL, LOW Level Input Voltage	MPU-6050	-0.5V to 0.3*VLOGIC	V	
VIH, HIGH-Level Input Voltage	MPU-6050	0.7*VLOGIC to VLOGIC + 0.5V	V	
Vhys, Hysteresis	MPU-6050	0.1*VLOGIC	V	
V_{OL1}, LOW-Level Output Voltage	3mA sink current	0 to 0.4	V	
I_{OL}, LOW-Level Output Current	V_{OL} = 0.4V	3	mA	
	V_{OL} = 0.6V	5	mA	
Output Leakage Current		100	nA	
t_{of}, Output Fall Time from V_{IHmax} to V_{ILmax}	C_b bus capacitance in pF	20+0.1C_b to 250	ns	
C_I, Capacitance for Each I/O pin		< 10	pF	
Auxiliary I^2C I/O (AUX_CL, AUX_DA)	**MPU-6050: *AUX_VDDIO*=0**			
V_{IL}, LOW-Level Input Voltage		-0.5V to 0.3*VLOGIC	V	
V_{IH}, HIGH-Level Input Voltage		0.7*VLOGIC to VLOGIC + 0.5V	V	
V_{hys}, Hysteresis		0.1*VLOGIC	V	
V_{OL1}, LOW-Level Output Voltage	VLOGIC > 2V; 1mA sink current	0 to 0.4	V	
V_{OL3}, LOW-Level Output Voltage	VLOGIC < 2V; 1mA sink current	0 to 0.2*VLOGIC	V	
I_{OL}, LOW-Level Output Current	V_{OL} = 0.4V	1	mA	
	V_{OL} = 0.6V	1	mA	
Output Leakage Current		100	nA	
t_{of}, Output Fall Time from V_{IHmax} to V_{ILmax}	C_b bus capacitance in pF	20+0.1C_b to 250	ns	
C_I, Capacitance for Each I/O pin		< 10	pF	

6.6 Electrical Specifications, Continued

Typical Operating Circuit of Section 7.2, VDD = 2.375V-3.46V, VLOGIC (MPU-6050 only) = 1.8V±5% or VDD, T_A = 25°C

Parameters	Conditions	Min	Typical	Max	Units	Notes
INTERNAL CLOCK SOURCE	**CLK_SEL=0,1,2,3**					
Gyroscope Sample Rate, Fast	DLPFCFG=0 SAMPLERATEDIV = 0		8		kHz	
Gyroscope Sample Rate, Slow	DLPFCFG=1,2,3,4,5, or 6 SAMPLERATEDIV = 0		1		kHz	
Accelerometer Sample Rate			1		kHz	
Clock Frequency Initial Tolerance	CLK_SEL=0, 25°C	-5		+5	%	
	CLK_SEL=1,2,3; 25°C	-1		+1	%	
Frequency Variation over Temperature	CLK_SEL=0		-15 to +10		%	
	CLK_SEL=1,2,3		±1		%	
PLL Settling Time	CLK_SEL=1,2,3		1	10	ms	
EXTERNAL 32.768kHz CLOCK	**CLK_SEL=4**					
External Clock Frequency			32.768		kHz	
External Clock Allowable Jitter	Cycle-to-cycle rms		1 to 2		µs	
Gyroscope Sample Rate, Fast	DLPFCFG=0 SAMPLERATEDIV = 0		8.192		kHz	
Gyroscope Sample Rate, Slow	DLPFCFG=1,2,3,4,5, or 6 SAMPLERATEDIV = 0		1.024		kHz	
Accelerometer Sample Rate			1.024		kHz	
PLL Settling Time			1	10	ms	
EXTERNAL 19.2MHz CLOCK	**CLK_SEL=5**					
External Clock Frequency			19.2		MHz	
Gyroscope Sample Rate	Full programmable range	3.9		8000	Hz	
Gyroscope Sample Rate, Fast Mode	DLPFCFG=0 SAMPLERATEDIV = 0		8		kHz	
Gyroscope Sample Rate, Slow Mode	DLPFCFG=1,2,3,4,5, or 6 SAMPLERATEDIV = 0		1		kHz	
Accelerometer Sample Rate			1		kHz	
PLL Settling Time			1	10	ms	

6.7 I²C Timing Characterization

Typical Operating Circuit of Section 7.2, VDD = 2.375V-3.46V, VLOGIC (MPU-6050 only) = 1.8V±5% or VDD, T_A = 25°C

Parameters	Conditions	Min	Typical	Max	Units	Notes
I²C TIMING	**I²C FAST-MODE**					
f_{SCL}, SCL Clock Frequency				400	kHz	
$t_{HD.STA}$, (Repeated) START Condition Hold Time		0.6			µs	
t_{LOW}, SCL Low Period		1.3			µs	
t_{HIGH}, SCL High Period		0.6			µs	
$t_{SU.STA}$, Repeated START Condition Setup Time		0.6			µs	
$t_{HD.DAT}$, SDA Data Hold Time		0			µs	
$t_{SU.DAT}$, SDA Data Setup Time		100			ns	
t_r, SDA and SCL Rise Time	C_b bus cap. from 10 to 400pF	20+0.1C_b		300	ns	
t_f, SDA and SCL Fall Time	C_b bus cap. from 10 to 400pF	20+0.1C_b		300	ns	
$t_{SU.STO}$, STOP Condition Setup Time		0.6			µs	
t_{BUF}, Bus Free Time Between STOP and START Condition		1.3			µs	
C_b, Capacitive Load for each Bus Line			< 400		pF	
$t_{VD.DAT}$, Data Valid Time				0.9	µs	
$t_{VD.ACK}$, Data Valid Acknowledge Time				0.9	µs	

Note: Timing Characteristics apply to both Primary and Auxiliary I²C Bus

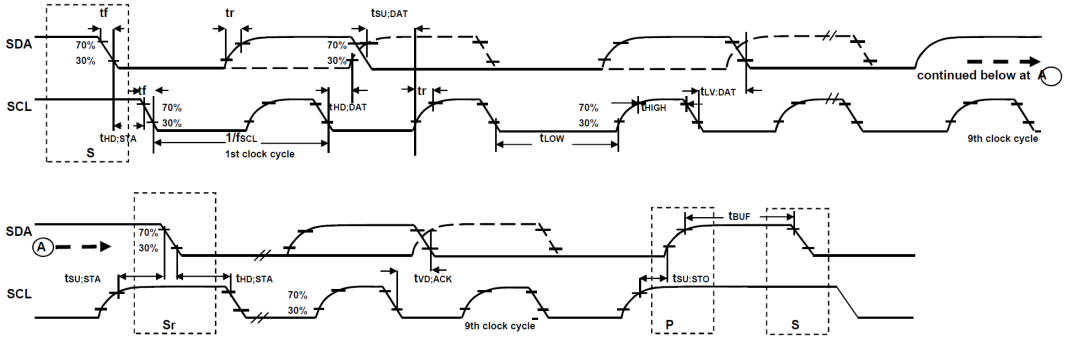

I²C Bus Timing Diagram

6.8 SPI Timing Characterization (MPU-6000 only)

Typical Operating Circuit of Section 7.2, VDD = 2.375V-3.46V, VLOGIC (MPU-6050 only) = 1.8V±5% or VDD, T_A = 25°C, unless otherwise noted.

Parameters	Conditions	Min	Typical	Max	Units	Notes
SPI TIMING						
f_{SCLK}, SCLK Clock Frequency				1	MHz	
t_{LOW}, SCLK Low Period		400			ns	
t_{HIGH}, SCLK High Period		400			ns	
$t_{SU.CS}$, CS Setup Time		8			ns	
$t_{HD.CS}$, CS Hold Time		500			ns	
$t_{SU.SDI}$, SDI Setup Time		11			ns	
$t_{HD.SDI}$, SDI Hold Time		7			ns	
$t_{VD.SDO}$, SDO Valid Time	C_{load} = 20pF			100	ns	
$t_{HD.SDO}$, SDO Hold Time	C_{load} = 20pF	4			ns	
$t_{DIS.SDO}$, SDO Output Disable Time				10	ns	

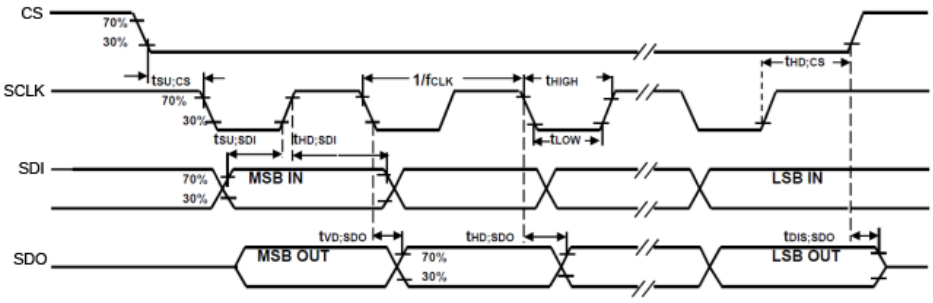

SPI Bus Timing Diagram

6.9 Absolute Maximum Ratings

Stress above those listed as “Absolute Maximum Ratings” may cause permanent damage to the device. These are stress ratings only and functional operation of the device at these conditions is not implied. Exposure to the absolute maximum ratings conditions for extended periods may affect device reliability.

Parameter	Rating
Supply Voltage, VDD	-0.5V to +6V
VLOGIC Input Voltage Level (MPU-6050)	-0.5V to VDD + 0.5V
REGOUT	-0.5V to 2V
Input Voltage Level (CLKIN, AUX_DA, AD0, FSYNC, INT, SCL, SDA)	-0.5V to VDD + 0.5V
CPOUT (2.5V ≤ VDD ≤ 3.6V)	-0.5V to 30V
Acceleration (Any Axis, unpowered)	10,000g for 0.2ms
Operating Temperature Range	-40°C to +105°C
Storage Temperature Range	-40°C to +125°C
Electrostatic Discharge (ESD) Protection	2kV (HBM); 250V (MM)
Latch-up	JEDEC Class II (2),125°C ±100mA

7 Applications Information

7.1 Pin Out and Signal Description

Pin Number	MPU-6000	MPU-6050	Pin Name	Pin Description
1	Y	Y	CLKIN	Optional external reference clock input. Connect to GND if unused.
6	Y	Y	AUX_DA	I^2C master serial data, for connecting to external sensors
7	Y	Y	AUX_CL	I^2C Master serial clock, for connecting to external sensors
8	Y		/CS	SPI chip select (0=SPI mode)
8		Y	VLOGIC	Digital I/O supply voltage
9	Y		AD0 / SDO	I^2C Slave Address LSB (AD0); SPI serial data output (SDO)
9		Y	AD0	I^2C Slave Address LSB (AD0)
10	Y	Y	REGOUT	Regulator filter capacitor connection
11	Y	Y	FSYNC	Frame synchronization digital input. Connect to GND if unused.
12	Y	Y	INT	Interrupt digital output (totem pole or open-drain)
13	Y	Y	VDD	Power supply voltage and Digital I/O supply voltage
18	Y	Y	GND	Power supply ground
19, 21	Y	Y	RESV	Reserved. Do not connect.
20	Y	Y	CPOUT	Charge pump capacitor connection
22	Y	Y	RESV	Reserved. Do not connect.
23	Y		SCL / SCLK	I^2C serial clock (SCL); SPI serial clock (SCLK)
23		Y	SCL	I^2C serial clock (SCL)
24	Y		SDA / SDI	I^2C serial data (SDA); SPI serial data input (SDI)
24		Y	SDA	I^2C serial data (SDA)
2, 3, 4, 5, 14, 15, 16, 17	Y	Y	NC	Not internally connected. May be used for PCB trace routing.

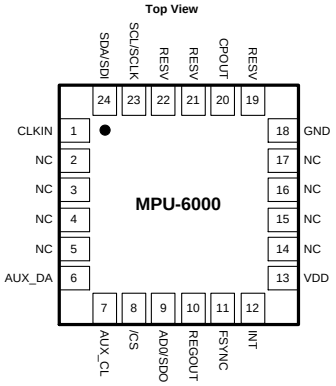

QFN Package
24-pin, 4mm x 4mm x 0.9mm

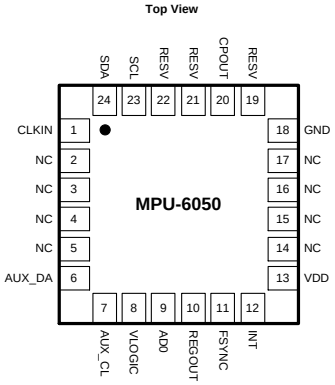

QFN Package
24-pin, 4mm x 4mm x 0.9mm

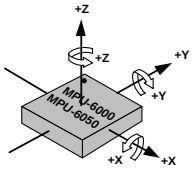

Orientation of Axes of Sensitivity and Polarity of Rotation

7.2 Typical Operating Circuit

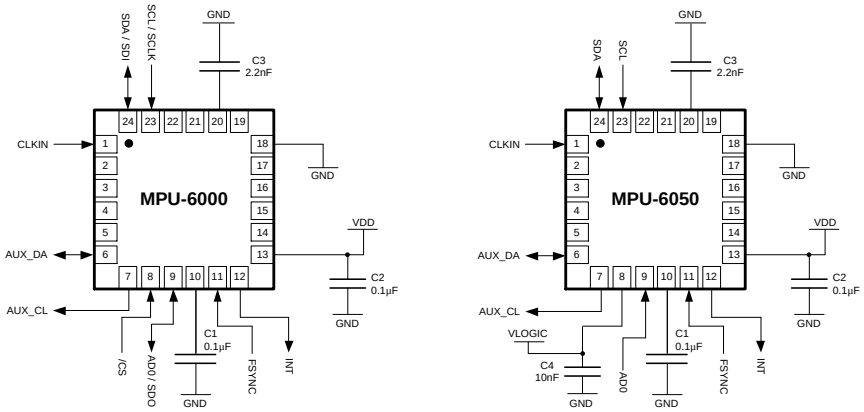

Typical Operating Circuits

7.3 Bill of Materials for External Components

Component	Label	Specification	Quantity
Regulator Filter Capacitor (Pin 10)	C1	Ceramic, X7R, 0.1µF ±10%, 2V	1
VDD Bypass Capacitor (Pin 13)	C2	Ceramic, X7R, 0.1µF ±10%, 4V	1
Charge Pump Capacitor (Pin 20)	C3	Ceramic, X7R, 2.2nF ±10%, 50V	1
VLOGIC Bypass Capacitor (Pin 8)	C4*	Ceramic, X7R, 10nF ±10%, 4V	1

* MPU-6050 Only.

7.4 Recommended Power-on Procedure

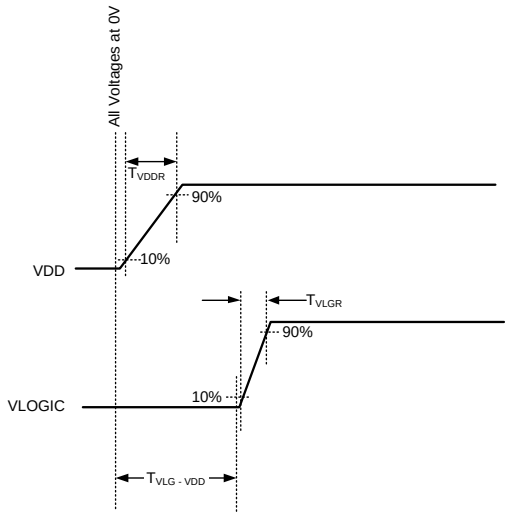

Power-Up Sequencing

1. VLOGIC amplitude must always be ≤VDD amplitude
2. T_{VDDR} is VDD rise time: Time for VDD to rise from 10% to 90% of its final value
3. T_{VDDR} is ≤100ms
4. T_{VLGR} is VLOGIC rise time: Time for VLOGIC to rise from 10% to 90% of its final value
5. T_{VLGR} is ≤3ms
6. $T_{VLG-VDD}$ is the delay from the start of VDD ramp to the start of VLOGIC rise
7. $T_{VLG-VDD}$ is ≥0
8. VDD and VLOGIC must be monotonic ramps

A.3 MAX6682 datasheet

19-2219; Rev 0; 2/02

MAXIM

Thermistor-to-Digital Converter

MAX6682

General Description

The MAX6682 converts an external thermistor's temperature-dependent resistance directly into digital form. The thermistor and an external fixed resistor form a voltage-divider that is driven by the MAX6682's internal voltage reference. The MAX6682 measures the voltage across the external resistor and produces a 10-bit + sign output code dependent on that voltage.

The MAX6682 does not linearize the highly nonlinear transfer function of a typical negative temperature coefficient (NTC) thermistor, but it does provide linear output data over limited temperature ranges when used with an external resistor of the correct value. Over the 0° to +50°C temperature range, the MAX6682 produces output data that is scaled to 8LSBs/°C (for 0.125°C resolution), provided that the correct thermistor and external resistor values are used. Other temperature ranges can be easily accommodated, but do not necessarily yield data scaled to an even number of LSBs per degree.

The 3-wire SPI™-compatible interface can be readily connected to a variety of microcontrollers.

The MAX6682 is a read-only device, simplifying use in systems where only temperature data is required.

Power-management circuitry reduces the average thermistor current, minimizing self-heating. Between conversions, supply current is reduced to 21µA (typ). The internal voltage reference is shut down between measurements.

The MAX6682 is available in a small, 8-pin µMAX package and is specified over the -55°C to +125°C temperature range.

Applications

HVAC

Medical Devices

Battery Packs/Chargers

Home Appliances

Pin Configuration appears at end of data sheet.

SPI is a trademark of Motorola, Inc.

Features

- **Converts Thermistor Temperature to Digital Data**
- **Low Average Thermistor Current Minimizes Self-Heating Errors**
- **Low Supply Current, 21µA (typ) Including 10kΩ Thermistor Current**
- **Internal Voltage Reference Isolates Thermistor from Power-Supply Noise**
- **10-Bit Resolution**
- **Accommodates Any Thermistor Temperature Range**
- **Output Data Scaled for Direct Temperature Readings from 0°C to +50°C**
- **Simple SPI-Compatible Interface**
- **Small, 8-Pin µMAX Package**

Ordering Information

PART	TEMP RANGE	PIN-PACKAGE
MAX6682MUA	-55°C to +125°C	8 µMAX

Typical Operating Circuit

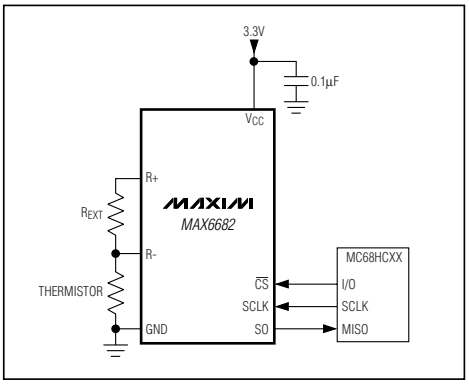

Thermistor-to-Digital Converter

MAX6682

ABSOLUTE MAXIMUM RATINGS

Supply Voltage (V_{CC} to GND) .....-0.3V to +6V
SO, SCK, $\overline{CS}$, R-, R+ to GND .....-0.3V to (V_{CC} + 0.3V)
R+ Current .....±20mA
R- Current .....±1mA
SCK, $\overline{CS}$, SO Current .....-1mA to +50mA
ESD Protection (Human Body Model) .....±2000V

Continuous Power Dissipation (T_A = +70°C)
8-Pin µMAX (derate 4.1mW/°C above +70°C) 328mW
Operating Temperature Range
(T_{MIN} to T_{MAX}) .....-55°C to +125°C
Storage Temperature Range .....-65°C to +150°C
Junction Temperature .....+150°C

Stresses beyond those listed under "Absolute Maximum Ratings" may cause permanent damage to the device. These are stress ratings only, and functional operation of the device at these or any other conditions beyond those indicated in the operational sections of the specifications is not implied. Exposure to absolute maximum rating conditions for extended periods may affect device reliability.

ELECTRICAL CHARACTERISTICS

(V_{CC} = 3V to 5.5V, T_A = -55°C to +125°C, unless otherwise noted. Typical values are specified at V_{CC} = 3.3V and T_A = +25°C.) (Note 1)

PARAMETER	SYMBOL	CONDITIONS	MIN	TYP	MAX	UNITS
Supply Voltage	V_{CC}		3.0		5.5	V
ADC Total Unadjusted Error	TUE	DOUT = 768.935 x (V_{REXT}/V_{R+}) - 134.0923; $V_{IN} > 0.1V_{REF}$	-3		+3	LSB
ADC Conversion Time	t_{CONV}			64	80	ms
R- Input Impedance	Z_{IN}		1			MΩ
R- Leakage Current				1	50	nA
Conversion Rate				0.5		Hz
Reference Voltage Output	V_{REF}	I_{LOAD} = 1mA	1.10	1.22	1.40	V
Reference Load Regulation		0 < I_{LOAD} < 2mA	0		0.1	%/mA
Reference Supply Regulation				0.7		mV/V
Conversion Supply Current	I_C	During conversion, no load		220	300	µA
Average Supply Current	I_A	0.5 conversions/s, no load		17	29	µA
Standby Current	I_S	$\overline{CS}$ low, SCK inactive		3	7	µA
Idle Current	I_{ID}	$\overline{CS}$ high, analog circuits off		10	17	µA
SERIAL INTERFACE						
Input Low Voltage	V_{IL}				0.2 x V_{CC}	V
Input High Voltage	V_{IH}		0.8 x V_{CC}			V
Input Leakage Current	I_{LEAK}	V_{IN} = GND or V_{CC}			1	µA
Output High Voltage	V_{OH}	I_{SOURCE} = 1.6mA	V_{CC} - 0.4			V
Output Low Voltage	V_{OL}	I_{SINK} = 1.6mA			0.4	V

TIMING CHARACTERISTICS

(V_{CC} = 3V to 5.5V, T_A = T_{MIN} to T_{MAX}, unless otherwise noted. Typical values are specified at V_{CC} = 3.3V and T_A = +25°C.) (Note 2)

PARAMETER	SYMBOL	CONDITIONS	MIN	TYP	MAX	UNITS
SERIAL INTERFACE TIMING (Figures 5 and 6)						
Serial Clock Frequency	fSCL				5	MHz
SCK Pulse High Width	tCH		50			ns
SCK Pulse Low Width	tCL		50			ns
CS Fall to SCK Rise	tCSS		35			ns
CS Fall to Output Data Valid	tDV	C_L = 10pF			35	ns
SCK Fall to Output Data Valid	tDO	C_L = 10pF			35	ns
CS Rise to Output High-Z	tTR	C_L = 10pF			25	ns
SCK Fall to Output High-Z	tHIZ	C_L = 10pF			35	ns
CS Pulse Width	tCSW		75			ns

Note 1: All specifications are 100% tested at T_A = +25°C. Specification limits over temperature are guaranteed by design, not production tested.

Note 2: Guaranteed by design.

Typical Operating Characteristics

(V_{CC} = 5V, thermistor = 10k nominal, R_{EXT} = 7680Ω, T_A = +25°C, unless otherwise noted.)

TEMPERATURE ERROR vs. POWER-SUPPLY NOISE FREQUENCY

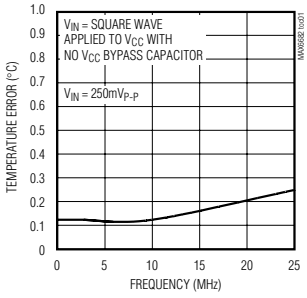

AVERAGE SUPPLY CURRENT vs. CLOCK FREQUENCY

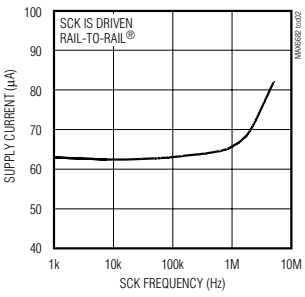

AVERAGE SUPPLY CURRENT vs. SUPPLY VOLTAGE

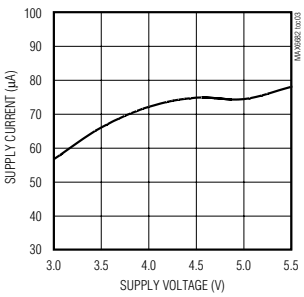

Rail-to-Rail is a registered trademark of Nippon Motorola, Ltd.

Thermistor-to-Digital Converter

Pin Description

PIN	NAME	FUNCTION
1	I.C.	Internally Connected. Connect to GND or leave unconnected.
2	R+	Reference Voltage Output. External resistor positive input.
3	R-	External Resistor Negative Input. Connect R- to the junction of the external resistor and the thermistor.
4	GND	Ground. Ground connection for MAX6682 and ground return for external thermistor.
5	$\overline{CS}$	Chip Select. Drive $\overline{CS}$ low to enable the serial interface.
6	SO	Serial Data Output
7	SCK	Serial Clock Input
8	V_{CC}	Positive Supply. Bypass V_{CC} to GND with a 0.1µF capacitor.

Detailed Description

The MAX6682 is a sophisticated interface circuit that energizes a low-cost thermistor and converts its temperature-dependent resistance to 10-bit digital data. The MAX6682 powers the thermistor only when a measurement is being made; the power dissipated in the thermistor is minimized. This virtually eliminates self-heating, a major component of thermistor error. The simple serial interface is compatible with common microcontrollers.

Temperature Conversion

The MAX6682 converts the voltage drop across the resistor R_{EXT} to a digital output using an internal 10-bit ADC. By measuring the voltage across R_{EXT}, the output code is directly related to temperature when using an NTC thermistor.

Although the relationship between a thermistor's resistance and its temperature is very nonlinear, the voltage across R_{EXT} is reasonably linear over a limited temperature range, provided that R_{EXT} is chosen properly. For example, over a +10°C to +40°C range, the relationship between the voltage across R_{EXT} and temperature is linear to within approximately 0.2°C. Wider temperature ranges result in larger errors.

The digital output is available as a 10-bit + sign word. The relationship between the 11-bit digital word and the voltage across R_{EXT} (normalized to V_{R+}) is given by:

$$D_{OUT} = \frac{\left(\frac{V_{REXT}}{V_{R+}} - 0.174387\right) \times 8}{0.010404}$$

where V_{REXT}/V_{R+} is the voltage across R_{EXT} normalized to the value of V_{R+}.

Table 1 shows the relationship between the voltage across R_{EXT} and the MAX6682's digital output code. It also shows the temperature that would produce the listed value of V_{REXT} when a standard thermistor is used in conjunction with R_{EXT} = 7680Ω. The MAX6682 produces output codes scaled to the actual temperature when used with the standard thermistor and R_{EXT} = 7680Ω over the +10°C to +40°C temperature range. Under these conditions, the nominal accuracy is about 0.2°C between +10° and +40°C, and about 1.5°C from 0°C to +50°C. In Table 1, the 3LSBs of the output code represent fractional temperatures. The LSB has a value of 0.125°C.

All table entries assume no errors in the values of R_{EXT} or the thermistor resistance. Table 1 also assumes the use of one of the following standard thermistors: Betatherm 10K3A1, Dale 1M1002, or Thermometrics C100Y103J. These thermistors have a nominal resistance of 10kΩ at +25°C and very similar temperature-to-resistance functions. They give the results shown in Table 1.

Different temperature ranges can be accommodated as well using different values of R_{EXT} (see *Choosing the External Resistor*). The MAX6682 works with thermistors other than the ones listed above, but the transfer functions vary somewhat.

Applications Information

Thermistors and Thermistor Selection

NTC thermistors are resistive temperature sensors whose resistance decreases with increasing temperature. They are available in a wide variety of packages that are useful in difficult applications such as measurement of air or liquid temperature. Some can operate over temperature ranges beyond that of most ICs. The relationship between temperature and resistance in an

Table 1. Temperature vs. Digital Output for Standard Thermistor with R_{EXT} = 7680Ω

THERMISTOR TEMPERATURE (°C)	V_{REXT} (mV) WITH STANDARD THERMISTOR AND R_{EXT} = 7680Ω*	DECIMAL VALUE OF D_{OUT} (1LSB = 0.125°C)	D_{OUT}
+60.000	921.6	+55.875	001 1011 1111
+50.000	830.6	+48.625	001 1000 0101
+40.000	720.5	+40.000	001 0100 0000
+30.000	595.4	+30.125	000 1111 0001
+25.000	530.1	+25.000	000 1100 1000
+20.000	464.4	+19.875	000 1001 1111
+10.000	339.7	+10.000	000 0101 0000
0	232.3	+1.500	000 0000 1100
-0.725	225.5	+1.000	000 0000 1000
-2.000	213.6	0.125	000 0000 0001
-5.000	187.4	-2.000	111 1111 0000

**Assumes V_{R+} = 1.220V.*

NTC thermistor is very nonlinear and can be described by the following approximation:

$$1 / T = A + B\ln R + C(\ln R)^3$$

where T is absolute temperature, R is the thermistor's resistance, and A, B, and C are coefficients that vary with manufacturer and material characteristics. The general shape of the curve is shown in Figure 1.

The highly nonlinear relationship between temperature and resistance in an NTC thermistor makes it somewhat more difficult to use than a digital-output temperature sensor IC, for example. However, by connecting the thermistor in series with a properly chosen resistor and using the MAX6682 to measure the voltage across the resistor, a reasonably linear transfer function can be obtained over a limited temperature range. Errors decrease for smaller temperature ranges.

Figures 2 and 3 show typical thermistor nonlinearity curves for a standard thermistor in conjunction with series resistors chosen to optimize linearity over two different temperature ranges: +10°C to +40°C and 0°C to +70°C.

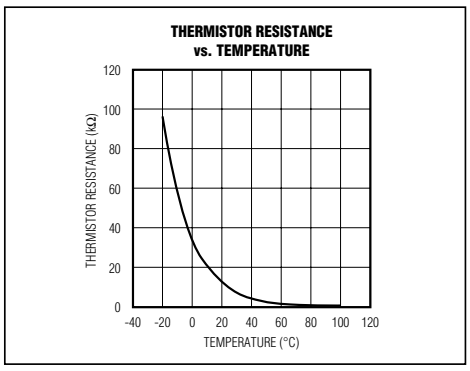

Figure 1. Thermistor Resistance vs. Temperature

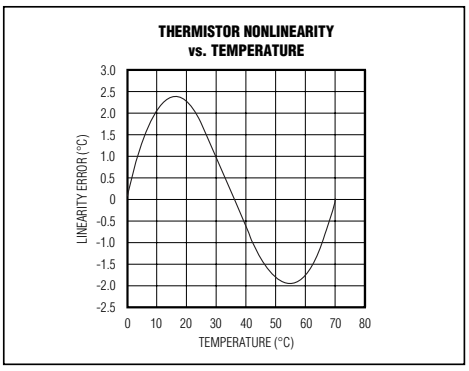

Figure 2. Thermistor Nonlinearity vs. Temperature for a Standard Thermistor from 0°C to +70°C

Thermistor-to-Digital Converter

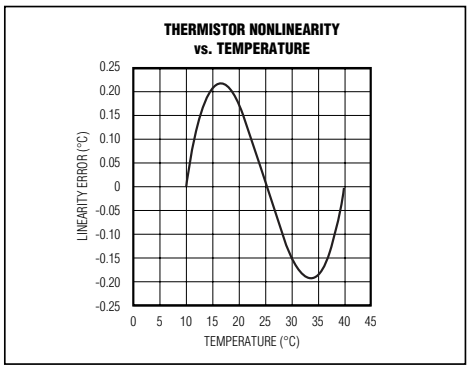

Figure 3. Thermistor Nonlinearity vs. Temperature for a Standard Thermistor from +10°C to +40°C

10-BIT TEMPERATURE READING											
Bit	10	9	8	7	6	5	4	3	2	1	0
	MSB (Sign)										LSB

Figure 4. SO Output

NTC thermistors are often described by the resistance at +25°C. Therefore, a 10kΩ thermistor has a resistance of 10kΩ at +25°C. When choosing a thermistor, ensure that the thermistor's minimum resistance (which occurs at the maximum expected operating temperature) in series with R_{EXT} does not cause the voltage reference output current to exceed about 1mA. Some standard 10kΩ thermistors with similar characteristics are listed in Table 2. When used with one of these thermistors and the recommended series resistor, the MAX6682 provides output data scaled in °C over the +10°C to +40°C temperature range.

Choosing the External Resistor

Choose R_{EXT} to minimize nonlinearity errors from the thermistor:

1) Decide on the temperature range of interest (for example 0°C to +70°C).
2) Find the thermistor values at the limits of the temperature range. R_{MIN} is the minimum thermistor value (at the maximum temperature) and R_{MAX} is the maximum thermistor value (at the minimum temperature). Also find R_{MID}, the thermistor resistance in the middle of the temperature range (+35°C for the 0°C to +70°C range).
3) Find R_{EXT} using the equation below:

$$R_{EXT} = \frac{R_{MID}(R_{MIN}+R_{MAX}) - 2R_{MIN}R_{MAX}}{R_{MIN}+R_{MAX}-2R_{MID}}$$

Table 3 shows nominal output data for several temperatures when R_{EXT} has been chosen according to the equation above for a temperature range of 0°C to +70°C. The output data is not conveniently scaled to the actual temperature over this range, but the linearity is better than 2.4°C over the 0°C to +70°C range (Figure 2). The temperature weighting over this range is 0.14925°C/LSB.

Serial Interface

The *Typical Application Circuit* shows the MAX6682 interfaced with a microcontroller. In this example, the MAX6682 processes the reading from R_{EXT} and transmits the data through an SPI-compatible interface. Force $\overline{CS}$ low and apply a clock signal at SCK to read the results at SO. Forcing $\overline{CS}$ low immediately stops any conversion in process. Initiate a new conversion by forcing $\overline{CS}$ high.

Force $\overline{CS}$ low to output the first bit on the SO pin. A complete read requires 11 clock cycles. Read the 11 output bits on the rising edge of the clock, if the first bit D10 is the sign bit. Bits D10–D0 contain the converted temperature in the order of MSB to LSB.

After the 11th clock cycle, SO goes to a high-impedance state. SO remains high impedance until $\overline{CS}$ is pulsed high and brought back low. Figure 4 is the SO output.

Power-Supply Considerations

The MAX6682 accuracy is relatively unaffected by power-supply coupled noise. In most applications, bypass V_{CC} to GND by placing a 0.1µF ceramic bypass capacitor close to the supply pin of the devices.

Thermal Considerations

Self-heating degrades the temperature measurement accuracy of thermistors. The amount of self-heating depends on the power dissipated in the thermistor and the dissipation constant of the thermistor. Dissipation constants depend on the thermistor's package and can vary considerably.

A typical thermistor might have a dissipation constant equal to 1mW/°C. For every mW the thermistor dissipates, its temperature rises by 1°C. For example, con-

sider a 10kΩ (at +25°C) NTC thermistor in series with a 5110Ω resistor operating at +40°C with a constant 5V bias. If it is one of the standard thermistors in Table 2, its resistance is 5325Ω at this temperature. The power dissipated in the thermistor is:

$$(5)^2(5325) / (5325 + 5110)^2 = 1.22mW$$

This thermistor would therefore have a self-heating error at +40°C of 1.22°C. Because the MAX6682 uses a small reference voltage and energizes the thermistor less than 2% of the time, the self-heating of the thermistor under the same conditions when used with the MAX6682 is only:

$$(1.22)^2(5325)(0.02) / (5325 + 5110)^2$$

=1.46µW, or only about 0.0015° (self-heating error)

Table 2. Standard Thermistors

MANUFACTURER	PART	WEBSITE
Betatherm	10K3A1	www.betatherm.com
Dale	1M1002	www.vishay.com/brands/dale/main.html
Thermometrics	C100Y103J	www.thermometrics.com

Table 3. Temperature vs. Digital Output for Standard Thermistor with R_{EXT} = 5110Ω

THERMISTOR TEMPERATURE (°C)	V_{REXT} (mV) WITH STANDARD THERMISTOR AND R_{EXT} = 5110Ω*	DECIMAL VALUE OF D_{OUT} (USING 1LSB = 0.125°C)	D_{OUT}
+75.000	946.0	57.75	001 1100 1110
+70.000	908.6	54.875	001 1011 0111
+60.000	820.6	47.875	001 0111 1111
+50.000	715.7	39.625	001 0011 1101
+40.000	597.4	30.25	000 1111 0010
+30.000	473.5	20.5	000 1010 0100
+25.000	412.6	15.750	000 0111 1110
+20.000	354.1	11.125	000 0101 1001
+10.000	249.2	2.875	000 0001 0111
0	165.1	-3.750	111 1110 0010
-5.000	131.5	-6.375	111 1100 1101

**Assumes V_{R+} = 1.220V.*

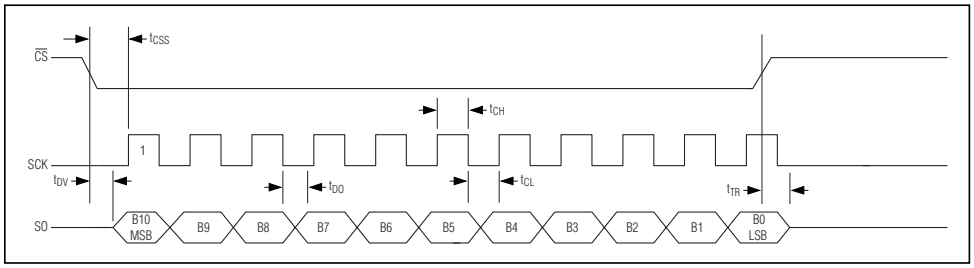

Figure 5. Serial Interface Timing

Thermistor-to-Digital Converter

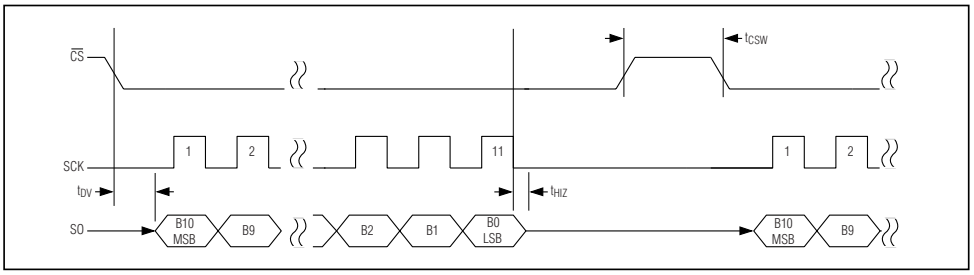

Figure 6. Serial Interface Timing 2

Functional Diagram

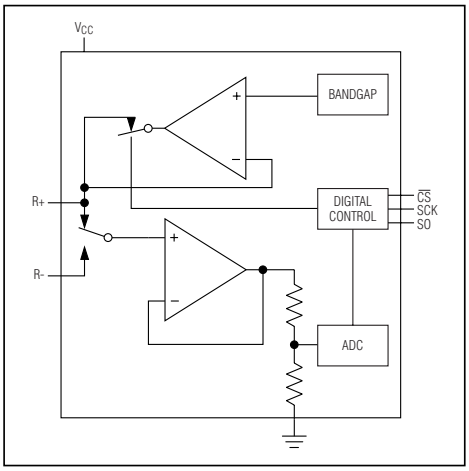

Pin Configuration

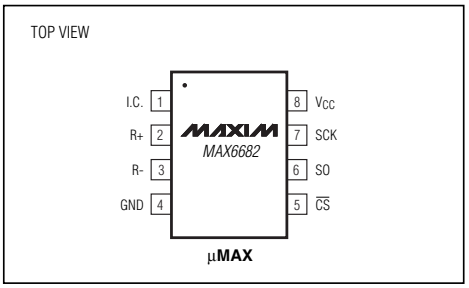

Chip Information

TRANSISTOR COUNT: 4909
PROCESS: BiCMOS

Package Information

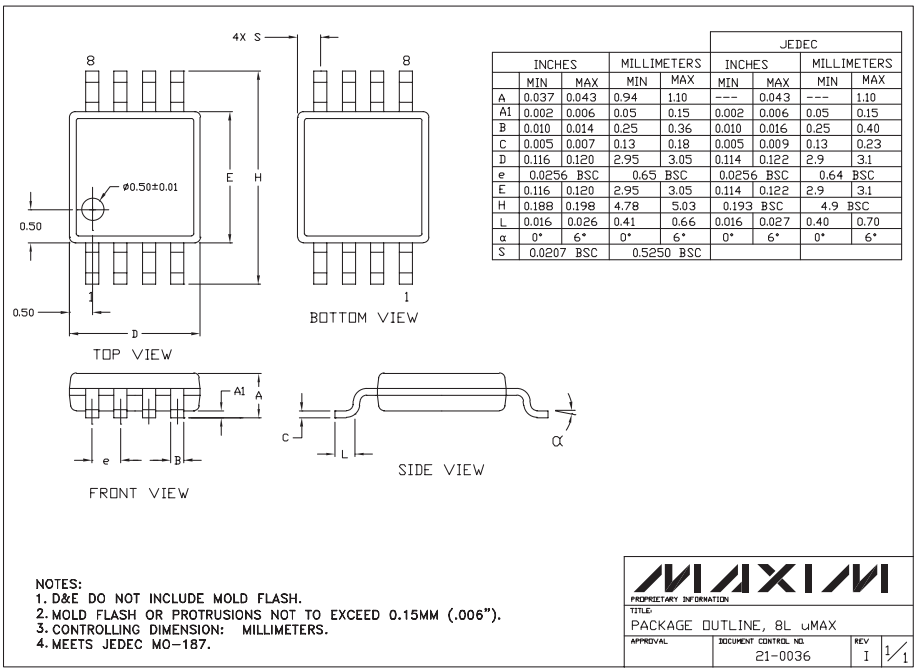

	INCHES		MILLIMETERS		JEDEC INCHES		JEDEC MILLIMETERS	
	MIN	MAX	MIN	MAX	MIN	MAX	MIN	MAX
A	0.037	0.043	0.94	1.10	---	0.043	---	1.10
A1	0.002	0.006	0.05	0.15	0.002	0.006	0.05	0.15
B	0.010	0.014	0.25	0.36	0.010	0.016	0.25	0.40
C	0.005	0.007	0.13	0.18	0.005	0.009	0.13	0.23
D	0.116	0.120	2.95	3.05	0.114	0.122	2.9	3.1
e	0.0256 BSC		0.65 BSC		0.0256 BSC		0.64 BSC	
E	0.116	0.120	2.95	3.05	0.114	0.122	2.9	3.1
H	0.188	0.198	4.78	5.03	0.193 BSC		4.9 BSC	
L	0.016	0.026	0.41	0.66	0.016	0.027	0.40	0.70
α	0°	6°	0°	6°	0°	6°	0°	6°
S	0.0207 BSC		0.5250 BSC					

NOTES:
1. D&E DO NOT INCLUDE MOLD FLASH.
2. MOLD FLASH OR PROTRUSIONS NOT TO EXCEED 0.15MM (.006").
3. CONTROLLING DIMENSION: MILLIMETERS.
4. MEETS JEDEC MO-187.

MAXIM
PROPRIETARY INFORMATION

TITLE: PACKAGE OUTLINE, 8L uMAX

APPROVAL	DOCUMENT CONTROL NO.	REV	
	21-0036	I	1/1

Appendix B

Arduino Code

B.1 Four piezo vibration sensors and IMU Code

```
// I2Cdev and MPU6050 must be installed as libraries, or else the .cpp/.h files
// for both classes must be in the include path of your project
#include "I2Cdev.h"
#include "MPU6050.h"

// Arduino Wire library is required if I2Cdev I2CDEV_ARDUINO_WIRE implementation
// is used in I2Cdev.h
#if I2CDEV_IMPLEMENTATION == I2CDEV_ARDUINO_WIRE
  #include "Wire.h"
#endif

// class default I2C address is 0x68
// specific I2C addresses may be passed as a parameter here
// AD0 low = 0x68 (default for InvenSense evaluation board)
// AD0 high = 0x69
MPU6050 accelgyro;
//MPU6050 accelgyro(0x69); // <-- use for AD0 high

int16_t ax, ay, az;
int16_t gx, gy, gz;

// uncomment "OUTPUT_READABLE_ACCELGYRO" if you want to see a tab-separated
// list of the accel X/Y/Z and then gyro X/Y/Z values in decimal. Easy to read,
// not so easy to parse, and slow(er) over UART.
#define OUTPUT_READABLE_ACCELGYRO

// uncomment "OUTPUT_BINARY_ACCELGYRO" to send all 6 axes of data as 16-bit
// binary, one right after the other. This is very fast (as fast as possible
// without compression or data loss), and easy to parse, but impossible to read
// for a human.
//#define OUTPUT_BINARY_ACCELGYRO

#define LED_PIN 13
bool blinkState = false;

const int F1_PIN = A0; // Piezo output
const int F2_PIN = A1;
const int L1_PIN = A2;
const int L2_PIN = A3;
void setup() {
  // join I2C bus (I2Cdev library doesn't do this automatically)
  #if I2CDEV_IMPLEMENTATION == I2CDEV_ARDUINO_WIRE
    Wire.begin();
  #elif I2CDEV_IMPLEMENTATION == I2CDEV_BUILTIN_FASTWIRE
    Fastwire::setup(400, true);
  #endif
```

```
    // initialize serial communication
    // (38400 chosen because it works as well at 8MHz as it does at 16MHz, but
    // it's really up to you depending on your project)
    Serial.begin(115200);

    // initialize device
    Serial.println("Initializing I2C devices...");
    accelgyro.initialize();

    // verify connection
    Serial.println("Testing device connections...");
    Serial.println(accelgyro.testConnection() ? "MPU6050 connection successful" : "MPU6050 connection
failed");

    // use the code below to change accel/gyro offset values
    /*
    Serial.println("Updating internal sensor offsets...");
    // -76 -2359    1688    0       0       0
    Serial.print(accelgyro.getXAccelOffset()); Serial.print("\t"); // -76
    Serial.print(accelgyro.getYAccelOffset()); Serial.print("\t"); // -2359
    Serial.print(accelgyro.getZAccelOffset()); Serial.print("\t"); // 1688
    Serial.print(accelgyro.getXGyroOffset()); Serial.print("\t"); // 0
    Serial.print(accelgyro.getYGyroOffset()); Serial.print("\t"); // 0
    Serial.print(accelgyro.getZGyroOffset()); Serial.print("\t"); // 0
    Serial.print("\n");
    accelgyro.setXGyroOffset(220);
    accelgyro.setYGyroOffset(76);
    accelgyro.setZGyroOffset(-85);
    Serial.print(accelgyro.getXAccelOffset()); Serial.print("\t"); // -76
    Serial.print(accelgyro.getYAccelOffset()); Serial.print("\t"); // -2359
    Serial.print(accelgyro.getZAccelOffset()); Serial.print("\t"); // 1688
    Serial.print(accelgyro.getXGyroOffset()); Serial.print("\t"); // 0
    Serial.print(accelgyro.getYGyroOffset()); Serial.print("\t"); // 0
    Serial.print(accelgyro.getZGyroOffset()); Serial.print("\t"); // 0
    Serial.print("\n");
    */

    // configure Arduino LED for
    pinMode(LED_PIN, OUTPUT);
}

void loop() {
    // read raw accel/gyro measurements from device
    accelgyro.getMotion6(&ax, &ay, &az, &gx, &gy, &gz);
```

```
    // these methods (and a few others) are also available
    //accelgyro.getAcceleration(&ax, &ay, &az);
    //accelgyro.getRotation(&gx, &gy, &gz);

    int piezoF1 = analogRead(F1_PIN);
    float F1_V = piezoF1 / 1023.0 * 5.0000;
    int piezoF2 = analogRead(F2_PIN);
    float F2_V = piezoF2 / 1023.0 * 5.0000;
    int piezoL1 = analogRead(L1_PIN);
    float L1_V = piezoL1 / 1023.0 * 5.0000;
    int piezoL2 = analogRead(L2_PIN);
    float L2_V = piezoL2 / 1023.0 * 5.0000;

    #ifdef OUTPUT_READABLE_ACCELGYRO
      // display tab-separated accel/gyro x/y/z values
      //Serial.print("a/g:\t");
      Serial.print(micros()); Serial.print("\t");
      Serial.print(ax); Serial.print("\t");
      Serial.print(ay); Serial.print("\t");
      Serial.print(az); Serial.print("\t");
      Serial.print(gx); Serial.print("\t");
      Serial.print(gy); Serial.print("\t");
      Serial.print(gz); Serial.print("\t");
      Serial.print(F1_V,5); Serial.print("\t");
      Serial.print(F2_V,5); Serial.print("\t");
      Serial.print(L1_V,5); Serial.print("\t");
      Serial.println(L2_V,5);
    #endif

    #ifdef OUTPUT_BINARY_ACCELGYRO
      Serial.write((uint8_t)(ax >> 8)); Serial.write((uint8_t)(ax & 0xFF));
      Serial.write((uint8_t)(ay >> 8)); Serial.write((uint8_t)(ay & 0xFF));
      Serial.write((uint8_t)(az >> 8)); Serial.write((uint8_t)(az & 0xFF));
      Serial.write((uint8_t)(gx >> 8)); Serial.write((uint8_t)(gx & 0xFF));
      Serial.write((uint8_t)(gy >> 8)); Serial.write((uint8_t)(gy & 0xFF));
      Serial.write((uint8_t)(gz >> 8)); Serial.write((uint8_t)(gz & 0xFF));
    #endif

    // blink LED to indicate activity
    blinkState = !blinkState;
    digitalWrite(LED_PIN, blinkState);
}
```

B.2 Two piezo vibration sensors and IMU Code

```
// I2Cdev and MPU6050 must be installed as libraries, or else the .cpp/.h files
// for both classes must be in the include path of your project
#include "I2Cdev.h"
#include "MPU6050.h"

// Arduino Wire library is required if I2Cdev I2CDEV_ARDUINO_WIRE implementation
// is used in I2Cdev.h
#if I2CDEV_IMPLEMENTATION == I2CDEV_ARDUINO_WIRE
  #include "Wire.h"
#endif

// class default I2C address is 0x68
// specific I2C addresses may be passed as a parameter here
// AD0 low = 0x68 (default for InvenSense evaluation board)
// AD0 high = 0x69
MPU6050 accelgyro;
//MPU6050 accelgyro(0x69); // <-- use for AD0 high

int16_t ax, ay, az;
int16_t gx, gy, gz;

// uncomment "OUTPUT_READABLE_ACCELGYRO" if you want to see a tab-separated
// list of the accel X/Y/Z and then gyro X/Y/Z values in decimal. Easy to read,
// not so easy to parse, and slow(er) over UART.
#define OUTPUT_READABLE_ACCELGYRO

// uncomment "OUTPUT_BINARY_ACCELGYRO" to send all 6 axes of data as 16-bit
// binary, one right after the other. This is very fast (as fast as possible
// without compression or data loss), and easy to parse, but impossible to read
// for a human.
//#define OUTPUT_BINARY_ACCELGYRO

#define LED_PIN 13
bool blinkState = false;

const int F1_PIN = A0; // Piezo output
const int F2_PIN = A1;
void setup() {
  // join I2C bus (I2Cdev library doesn't do this automatically)
  #if I2CDEV_IMPLEMENTATION == I2CDEV_ARDUINO_WIRE
    Wire.begin();
  #elif I2CDEV_IMPLEMENTATION == I2CDEV_BUILTIN_FASTWIRE
    Fastwire::setup(400, true);
  #endif
  // initialize serial communication
  // (38400 chosen because it works as well at 8MHz as it does at 16MHz, but
```

```
    // it's really up to you depending on your project)
    Serial.begin(115200);

    // initialize device
    Serial.println("Initializing I2C devices...");
    accelgyro.initialize();

    // verify connection
    Serial.println("Testing device connections...");
    Serial.println(accelgyro.testConnection() ? "MPU6050 connection successful" : "MPU6050 connection
failed");

    // use the code below to change accel/gyro offset values
    /*
    Serial.println("Updating internal sensor offsets...");
    // -76 -2359    1688    0          0          0
    Serial.print(accelgyro.getXAccelOffset()); Serial.print("\t"); // -76
    Serial.print(accelgyro.getYAccelOffset()); Serial.print("\t"); // -2359
    Serial.print(accelgyro.getZAccelOffset()); Serial.print("\t"); // 1688
    Serial.print(accelgyro.getXGyroOffset()); Serial.print("\t"); // 0
    Serial.print(accelgyro.getYGyroOffset()); Serial.print("\t"); // 0
    Serial.print(accelgyro.getZGyroOffset()); Serial.print("\t"); // 0
    Serial.print("\n");
    accelgyro.setXGyroOffset(220);
    accelgyro.setYGyroOffset(76);
    accelgyro.setZGyroOffset(-85);
    Serial.print(accelgyro.getXAccelOffset()); Serial.print("\t"); // -76
    Serial.print(accelgyro.getYAccelOffset()); Serial.print("\t"); // -2359
    Serial.print(accelgyro.getZAccelOffset()); Serial.print("\t"); // 1688
    Serial.print(accelgyro.getXGyroOffset()); Serial.print("\t"); // 0
    Serial.print(accelgyro.getYGyroOffset()); Serial.print("\t"); // 0
    Serial.print(accelgyro.getZGyroOffset()); Serial.print("\t"); // 0
    Serial.print("\n");
    */

    // configure Arduino LED for
    pinMode(LED_PIN, OUTPUT);
}

void loop() {
    // read raw accel/gyro measurements from device
    accelgyro.getMotion6(&ax, &ay, &az, &gx, &gy, &gz);


    // these methods (and a few others) are also available
    //accelgyro.getAcceleration(&ax, &ay, &az);
```

```
    //accelgyro.getRotation(&gx, &gy, &gz);

    int piezoF1 = analogRead(F1_PIN);
    float F_V = piezoF1 / 1023.0 * 5.0000;
    int piezoF2 = analogRead(F2_PIN);
    float F_H = piezoF2 / 1023.0 * 5.0000;

    #ifdef OUTPUT_READABLE_ACCELGYRO
        // display tab-separated accel/gyro x/y/z values
        //Serial.print("a/g:\t");
        Serial.print(micros()); Serial.print("\t");
        Serial.print(ax); Serial.print("\t");
        Serial.print(ay); Serial.print("\t");
        Serial.print(az); Serial.print("\t");
        Serial.print(gx); Serial.print("\t");
        Serial.print(gy); Serial.print("\t");
        Serial.print(gz); Serial.print("\t");
        Serial.print(F_V,5); Serial.print("\t");
        Serial.println(F_H,5)
    #endif

    #ifdef OUTPUT_BINARY_ACCELGYRO
        Serial.write((uint8_t)(ax >> 8)); Serial.write((uint8_t)(ax & 0xFF));
        Serial.write((uint8_t)(ay >> 8)); Serial.write((uint8_t)(ay & 0xFF));
        Serial.write((uint8_t)(az >> 8)); Serial.write((uint8_t)(az & 0xFF));
        Serial.write((uint8_t)(gx >> 8)); Serial.write((uint8_t)(gx & 0xFF));
        Serial.write((uint8_t)(gy >> 8)); Serial.write((uint8_t)(gy & 0xFF));
        Serial.write((uint8_t)(gz >> 8)); Serial.write((uint8_t)(gz & 0xFF));
    #endif

    // blink LED to indicate activity
    blinkState = !blinkState;
    digitalWrite(LED_PIN, blinkState);
}
```

Appendix C

Connections

C.1 Connections in FRF

Color of the wire that comes out of the lateral case attached in the foot sole	**Arduino connection**
Brown	5V
Red	3.3V
Pink	GND
White	A0
Yellow	A1
Blue	SCL
Grey	SDA

Table C.1: Table that includes the connections made between the electronic circuit and the Arduino in the FRF.

C.2 Connections in FLF

Color of the wire that comes out of the lateral case attached in the foot sole	**Arduino connection**
Red	5V
Green	5V (A0)
Grey	GND
White	A1
Yellow	A2
Blue	CS (10)
Brown	MISO (12)
Pink	SCK (13)

Table C.2: Table that includes the connections made between the electronic circuit and the Arduino in the FLF.

Appendix D

Precision Agriculture

In the beginning of the project, precision agriculture was also considered as a field where the addition of sensors in the feet could help. A secondary objective included in the project was to use sensors that could allow the ANYmal performing soil analysis.

With this goal in mind, the Table D.1, was been prepared using [14] and [15] among others, in order to summarize the parameters to be considered in soil analysis. In the table all important parameters are included with: a small description including their importance, the optimal values for each parameter, the periodicity the samples should be taken, the depth in where the samples should be taken, the distance that should be considered between samples and the correlation with other properties.

From all these parameters, the fundamental ones are N, P, K, pH and EC. However, in the field only pH and EC can be measured and they should be measured in a depth of at least 15cm. The other parameters are quantified using samples, taken at a depth of at least 15cm, and lab methods which are far from being performed in the field.

In conclusion, the use of sensors integrated in the small feet of the ANYmal to develop soil analysis was from the beginning maybe too optimistic because of the difficulties of: using small sensors in the field and performing the measurements in a depth of more than 10cm in the ground without the use of any actuator.

Property	Description	Parameter	Units	Optimal values	Sample periodicity	Depth	Distance between samples	Correlation
Acidity or Soil reaction	Concentration of H^+ in the soil.	pH	-	6 - 7,3	4 Years	15 - 30 cm	12 samples/4 ha	-
Electrical Conductivity or Salinity	Soil electrical conductivity (EC) is a measurement that correlates with soil properties that affect crop productivity, including soil texture, drainage conditions, organic matter level, salinity, and subsoil characteristics.	EC	µS/cm	< 500	4 Years	15 - 30 cm	12 samples/4 ha	N, CEC, %OM
Nitrates or Nitrogen	Primary nutrient for plant groth, responsible for plants' green foliage. Over-applying can "burn" plants.	N	ppm	25 - 35 *	Anual	30-120cm	20 samples/4 ha	CE
Phosphorus	Primary nutrient and key element plants need for flowering, fruiting and rooting.	P (P_2O_5)	P Olsen ppm	0 - 75 *	4 Years	15 - 30 cm	12 samples/4 ha	-
Potassium	Potassium, as primary nutrient, is important for over-wintering ability of perennial crops, overall growth and longevity and disease resistance.	K (K_2O)	ppm	100 - 175 *	4 Years	15 - 30 cm	12 samples/4 ha	-
Magnesium	Magnesium it is used in plant photosyntesis if magnesium level is low dolomitic lime should be used to increase the soil pH.	Mg	kg/ha ppm	200 - 300 40 - 80	-	15 - 30 cm	12 samples/4 ha	pH
Calcium	Secondary macronutrient, plays a major role in plant cell structure and membrane integrity. It is also associated with many critical cellular functions.	Ca	ppm	1000-1600	-	15 - 30 cm	12 samples/4 ha	pH
Sulfur	Increase protein levels in grain crops, encourages formation of nodules in legume crops and give characteristic smell and tast of onions and garlic.	S	kg/ha	> 40	-	0 - 40 cm	12 samples/4 ha	-
Iron	Important for crops that prefer acid soils such blueberries, strawberries, grains, soybeans and col crops. It takes part in nitrogen-fixing in legume crops.	Fe	ppm	50 - 100	-	15 - 30 cm	12 samples/4 ha	-
Cation Exchange Capacity	It determines the capacity of the field to absorb cations of the provided fertilizer.	CEC	meq/100g	10 - 20 *	Initially	15 - 30 cm	-	pH
Soil Organic Matter	Consisting of plant and animal residues at various stages of descomposition. It increases soil fertility providing cation exchange sites and acting as reserve of plant nutrients (N, P, S).	% OM	%	> 3,5	4 Years	15 - 30 cm	12 samples/4 ha	N, P, S
Moisture / Soil Water Content / Field Capacity	Water contained in a volume of soil // Capacity of the field to retain water.	Moisture SWC FC (layer)	% m^3 wat/m^3 soil cm	*	Anually	15 - 120 cm	-	Density and porosity
Temperature	Physical quantity expressing hot and cold. The selection of the crops should depend on the climate. Another important parameter to be considered is soil temperature.	T	°C	18 - 24°C *	Daily	-	-	-
Soil Density	Surface soil density can be measured with a penetrometer and it is interesting to know the soil compaction.	ρ	g/cm^3	< 1,6 *	Initially	0 - 30 cm	-	Porosity

* Depending on the crops and the types of soil

Table D.1: This table summarizes all the important parameters to be considered while performing soil analysis.